HIGH-RESOLUTION ARRAY COMPARATIVE GENOMIC HYBRIDIZATION IDENTIFIES COMMON TARGETS IN RHABDOMYOSARCOMA

APPROVED BY SUPERVISORY COMMITTEE

_____
Scott Cameron, M.D. Ph.D. (mentor)

_____
James Amatruda, M.D. Ph.D. (chair)

_____
John Minna, M.D.

_____
Diego Castrillon, M.D. Ph.D.

_____
Rene Galindo, M.D. Ph.D.

DEDICATION

I dedicate this dissertation to the inspiration for my work, my much-missed mother, Annette Paulson; her strength, spirit, and determination have led me to become who I am today. I also wish to dedicate this dissertation to my father, Roger Paulson, and brother, Corey Paulson, for their unfailing love, support, and shared sense of humor. To the rest of my family, Monte, Rhonda, and Paige Runge, and to those friends who have become family, Judith and Earl LaFontaine, Laurie Creek, and Susan Barnes; along each step of this path, they have generously shared their wisdom and their hearts. As my mother would say, “I love you bunches and bunches.” To the teachers, colleagues, and students, that have helped me to find my love of genetics, my career path as an MD/PhD, and my passion for learning and knowledge, without your direction I would not have pursued my calling. Finally, I would like to thank my Thesis Committee and especially my mentor, Scott Cameron, as their guidance have made this project possible.

HIGH-RESOLUTION ARRAY COMPARATIVE GENOMIC HYBRIDIZATION IDENTIFIES COMMON TARGETS IN RHABDOMYOSARCOMA

BY

VERA ASHLEY PAULSON

DISSERTATION

Presented to the Faculty of the Graduate School of Biomedical Sciences

The University of Texas Southwestern Medical Center at Dallas

In Partial Fulfillment of the Requirements

For the Degree of

DOCTOR OF PHILOSOPHY

The University of Texas Southwestern Medical Center at Dallas

Dallas, Texas

June, 2010

HIGH-RESOLUTION ARRAY COMPARATIVE GENOMIC HYBRIDIZATION IDENTIFIES COMMON TARGETS IN RHABDOMYOSARCOMA

VERA ASHLEY PAULSON

The University of Texas Southwestern Medical Center at Dallas, 2010

SCOTT CAMERON M.D./Ph.D.

Rhabdomyosarcoma (RMS) accounts for nearly 50 percent of the soft tissue sarcomas that affect children. There are two major histological variants, alveolar (ARMS) and embryonal (ERMS). Both are defined as sarcomas that show exclusive evidence of muscle differentiation, but differ in their pathogenesis and prognosis. ARMS typically occurs in adolescents, presents as disease of the extremities, has a higher risk of metastasis or treatment-resistance, and in 75% of cases, is characterized by the presence of the *PAX3/7:FOXO1* translocation. ERMS is associated with a younger age at presentation, sites of disease other

than the extremities, a more favorable clinical outcome, and the absence of consistent chromosomal translocations. Here we used high-density array-based comparative genomic hybridization to examine the genomes of RMS to identify common programs that drive tumor pathogenesis.

TABLE OF CONTENTS

PRIOR PUBLICATIONS

Articles:

Paulson, Vera & Stanford, Amy. "Drosophila Melanogaster: A Model for Studying Human Disease." TAMU Undergraduate Journal of Science. Vol. 5 No. 1 / Spring 2004 34- 40.

Shalmica R Jackson , Chun-Hong Zhu , Vera Paulson , Linda Watkins , Z Gunnur Dikmen, Sergei M Gryaznov , Woodring E Wright , Jerry W Shay. "Antiadhesive Effects of GRN163L--An Oligonucleotide N3'->P5' Thio-Phosphoramidate Targeting Telomerase." Cancer Res. 2007 Feb 1;67 (3):1121-9 17283146.

Online publications:

Paulson, V. (2009, February 2). Case of the Week: Chordoma. University of Texas Southwestern Department of Pathology. [Online]. http://pathcuric1.swmed.edu/Teaching/COW/020209cow.htm.

Paulson, V. (2009, April 30) Case of the Week: Chordoma. University of Texas Southwestern Department of Pathology. [Online]. http://pathcuric1.swmed.edu/Teaching/COW/043009cow.htm.

Paulson, V and Ambruzs, J. (2009, August 10) Case of the Week: Oncocytic carcinoma. University of Texas Southwestern Department of Pathology. [Online]. http://pathcuric1.swmed.edu/Teaching/COW/081009cow.htm.

LIST OF FIGURES

LIST OF TABLES

LIST OF APPENDICES

LIST OF DEFINITIONS

aCGH: Array comparative genomic hybridization

ALL: Acute lymphoblastic leukemia

AKT: v-akt murine thymoma viral oncogene homolog 1

ARMS: Alveolar rhabdomyosarcoma

ATP: Adenosine tri-phosphate

BCL2L1: B-Cell lymphoma 2 like protein 1

BMI1: B lymphoma Mo-MLV insertion region 1 homolog, polycomb ring finger oncogene

CDK,4/5/6: Cyclin-dependent kinase, 4/5/6

CDKN1C: Cyclin-dependent kinase inhibitor 1C ($p57^{KIP2}$)

CDKN2A: Cyclin-dependent kinase inhibitor 2A ($p16^{INK4a}$/$p14^{ARF}$)

CDKN2B: Cyclin-dependent kinase inhibitor 2B ($p15^{INK4B}$)

CCDKN2D: Cyclin-dependent kinase inhibitor 2D ($p19^{INK4D}$)

CHTN: Cooperative human tissue network

CMCD: Children's Medical Center of Dallas

C-MET: met proto-oncogene (hepatocyte growth factor receptor)

CNV: Copy number variable

CNS: Central nervous system

COG: Children's Oncology Group

E12: transcription factor 3 (E2A immunoglobulin enhancer binding factors E12/E47)

EGFR: Epidermal growth factor receptor

ERK1/2: extracellular signal-regulated kinase 1/2

ERMS: Embryonal rhabdomyosarcoma

FFPE: Formalin-fixed paraffin embeded

FISH: Fluorescent in situ hybridization

FGFR1-4: Fibroblast growth factor 1-4

FOXO1: Forkhead

GDP/GTP: Guanosine di/tri-phosphate

GISTIC: Genomic identification of significant targets in cancer

GLI1-3: Zinc finger transcription factor homologous to cubitus interruptus

GSEA: Gene set enrichment analysis

H19: H19, imprinted maternally expressed transcript (non-protein coding)

HGF/SF: Hepatocyte growth factor/ scatter factor

HH: Hedgehog

HLH : Helix-loop-helix transcription factor

HOX: Homeodomain transcription factor

HRAS: v-Ha-ras Harvey rat sarcoma viral oncogene homolog

IGF2: Insulin like growth factor 2

IGFR1: Insulin like growth factor receptor 1

IHC: Immunohistochemistry

KRAS: v-Ki-ras2 Kirsten rat sarcoma viral oncogene homolog

mAb: Monoclonal Ab

MAPK: Mitogen-activated protein kinase, p38

MDM2: Mdm2 p53 binding protein homolog (mouse)

MEK: MAPK/ERK kinase kinase , mitogen-activated protein kinase kinase kinase 1

MLL: Mixed lineage leukemia

MRF: Myogenic regulatory factor

m-TOR: Mechanistic target of rapamycin (serine/threonine kinase)

MYOD: Myosin D

NF1: Neurofibromin

NRAS: neuroblastoma RAS viral (v-ras) oncogene homolog

NSCLC: Non-small cell lung cancer

PAX3: Paired box gene 3 (Waardenburg syndrome 1)

PAX7: Paired box homeotic gene 7

PBX: Pre-B-cell leukemia homeobox 1

PCR: Polymerase chain reaction

PI3K: Phosphoinositide-3-kinase, regulatory subunit 1 (alpha)

PNS: Peripheral nervous system

POU3F3: POU class 3 homeobox 3, brain-1

PTCH1: Patched1

PTEN: phosphatase and tensin homolog

PTPN11: protein tyrosine phosphatase, non-receptor type 11

QPCR: quantitative polymerase chain reaction

RASSF1: Ras association (RalGDS/AF-6) domain family member 1

RB: Retinoblastoma

RMS: Rhabdomyosarcoma

RNAi: RNA interference

SMO: Smoothened

SNET: DNA buffer (defined in methods)

SNPs: Single nucleotide polymorphisms

STAT3: Signal transcription and transducer 3

SUFU: Supressor of fused

TKI: Tyrosine kinase inhibitor

TUSC2: tumor suppressor candidate 2

WNT, 5a, 10b, 11: wingless-type MMTV integration site family, members 5a, 10b, 11

CHAPTER ONE: INTRODUCTION

RHABDOMYOSARCOMA:

Rhabdomyosarcoma (RMS) accounts for nearly 50 percent of the soft tissue sarcomas that affect children. There are two major histological variants, alveolar (ARMS) and embryonal (ERMS). Both are pathologically defined as sarcomas that show exclusive evidence of muscle differentiation by immunohistochemical and ultrastructural studies (Qualman et al. 1998). These tumors typically present in locations in or near muscle beds, but may also arise at sites that lack skeletal muscle, for example the biliary or genitourinary tract (Hettmer and Wagers 2010). Tumors range from poorly to well differentiated (Bridge et al. 2000), and by histology tumor cells appear to be small and round or oblong. Some of these cells exhibit cross-striations of a more differentiated muscle phenotype or multiple nuclei (Hettmer and Wagers 2010). Immunohistochemistry demonstrates a wide range of combinations and expression levels of muscle markers, including desmin, myosin, and several of the myogenic regulatory factors (MRFs), but staining for myosin D (MYOD) and myogenin (MYOG) alone, is sufficient for diagnosis of RMS, as it offers a sensitivity of 97 percent (De Giovanni et al. 2009).

Despite their proposed common origins in skeletal muscle, the two variants differ in their pathogenesis and prognosis (Qualman et al. 1998). ARMS makes up 20 percent of clinical cases, typically occurs in adolescents, presents as disease of the extremities, has a higher risk of metastasis or treatment-resistance, and is characterized by the presence of the *PAX3/7:FOXO1* translocation in 75% of cases. (Qualman et al. 1998; Xia et al. 2002). ERMS is more common and occurs in 70-80 percent of cases. ERMS is associated with a younger age at presentation (typically under 10 years old), sites of disease other than the extremities, a more favorable clinical outcome, and the absence of consistent chromosomal translocations (Qualman et al. 1998; Xia et al. 2002).

CLINICAL STRATIFICATION

Children with RMS are stratified into clinical groups (low, intermediate, and high) based on a complex combination of clinical and pathological factors including site and extent of disease at presentation, histology, and the success of surgical attempts to render the child disease free (Hayes-Jordan and Andrassy 2009). These clinical groups assist in determining treatment strategy (Oberlin et al. 2008). Children with disease stratified as low-risk, localized ERMS, have a cure rate of up to 95 percent (De Giovanni et al. 2009). For those children diagnosed with intermediate-

risk disease, the most common clinical presentation, one-third will likely relapse and die (Stevens et al. 2005). High-risk patients have a far more dismal outcome, with survival rates as low as 10-30 percent, in the case of metastatic ARMS (De Giovanni et al. 2009). For those patients that live, many suffer severe late effects of treatment including disfigurement (often as a consequence of high dose irradiation of growing tissue), organ toxicity, and premature death (Oeffinger et al. 2006; Punyko et al. 2005; Stevens et al. 2005). Thus, it follows that there is a need for the identification of novel targets that improved therapies can be directed against, and for the identification of biological markers to identify disease risk.

PRIOR STUDIES IN RMS

Previous studies in RMS have focused on a broad description of the tumor genomes, identifying common chromosomal and cytoband abnormalities through the use of low-resolution metaphase array comparative genomic hybridization (CGH) (Bridge et al. 2002; Bridge et al. 2000; Gordon et al. 2001; Pandita et al. 1999). The metaphase CGH platform, at best, offers a resolution of 5-10 Mb, and this has largely limited the studies to a catalogue of the frequency of chromosomal gains and losses and the identification of potential regions of interest containing

hundreds of genes (Pandita et al. 1999). The genomes of RMS are highly aneuploid or hyper-diploid and exhibit extensive structural abnormalities (Goldstein et al. 2006). There are frequent, but neither consistent nor specific, chromosomal gains or losses in ERMS or in addition to the *PAX3/7:FOXO1* translocations observed in ARMS (Goldstein et al. 2006). Interestingly, several of the observed regions amplified in ARMS are also in regions of chromosomal gain in ERMS (Gordon et al. 2001). While limited by low-resolution approaches these studies were still able to describe several intriguing examples of copy number aberrations including Insulin-like growth factor receptor-1 (*IGFR1*) amplifications and copy number abnormalities in the Hedgehog signaling pathway (Bridge et al. 2002).

Many cancers that affect adults have mutations in the “usual suspects” in cancer biology, and candidate approaches in the study of RMS have determined it is no different (Xia et al. 2002). Mutations in P53, loss of cell-cycle inhibitors or amplification of cyclin-dependent kinases, activation of the Ras pathway, and amplification of MYC-N (in approximately 40 percent of ARMS cases), have all been identified in RMS (Xia et al. 2002).

Recently, a large scale expression analysis of 160 RMS tumors, including ERMS, translocation-positive ARMS, and translocation-negative ARMS, as well as other soft-tissue sarcomas was completed (Davicioni et al. 2009). This study failed to cluster tumors by histology without a supervised analysis (Davicioni et al. 2009), suggesting that the genomic programs that drive ERMS and ARMS have a common foundation that is *modified* to generate the distinct histologies and clinical behaviors of the ERMS and ARMS subtypes. They also suggest that treatment approaches developed through the study of one histological subtype may apply more broadly, which is consistent with long standing clinical data demonstrating sensitivity of both histological subtypes to the common chemotherapy regimen currently in use (principally vinciristine, dactinomycin, and cyclophosphamide).

WHAT RMS POPULATION WOULD MOST BENEFIT FROM ADDITIONAL STUDY?

The heterogeneity of RMS, the inadequacy of current patient risk-stratification and treatment, and the potential for clinical impact were all considerations in determining which RMS population might benefit most from additional study.

While recent expression analysis would suggest that ERMS and ARMS have a common foundation that is *modified* to generate distinct histologies, other studies suggest that the two are molecularly distinct, a hypothesis supported by their disparity in both the clinical setting and the absence of the fusion translocation in ERMS. Thus, the decision was made to use a clinically homogenous group of tumors, as use of a narrowly defined subgroup would increase the likelihood of discovering novel pathways less reflective of histology, and more indicative of pathways involved in the biology of this tumor.

Our choice of intermediate-risk embryonal RMS took into consideration the relative deficiency of studies of ERMS and the fact that it represented the largest clinical subgroup that might benefit from better risk stratification and the identification of potential targets at which to direct novel therapeutics. The identification of biological markers of disease risk in the intermediate-risk group might potentially improve treatment by allowing more intensive therapy to be directed only to those children at higher risk of recurrence, while reducing therapy and attendant late effects of treatment for those likely to be cured.

CHOOSING A PLATFORM:

As noted above, a recent study of gene expression patterns in 160 RMS tumors has been completed (Davicioni et al. 2009), and a number groups are using this data to propose the presence of pathogenic candidates, molecular signatures, and potential prognostic markers. The expression data however, only covers 11,694 genes, leaving expression of half the genome unknown.

While previous studies of genomic copy number have been limited in identifying single genes, the technology for array CGH has advanced markedly in the intervening six years, and resolution has improved from 5-10 Mb to 5-10 kb.

THE PROPOSAL

It is our goal to define the genome of intermediate-risk embryonal RMS with the belief that there are recurrent DNA loci that when amplified or deleted in tumors increase the risk of recurrence. Some of these loci may have prognostic value, while others will offer potential therapeutic targets in the treatment of RMS.

CHAPTER TWO: CGH & ANALYSIS

INTRODUCTION

The development of drugs that target developmental and signaling pathways has become an important new approach to cancer therapeutics and requires the identification of pathways responsible for the pathogenesis of specific tumor types. To define the genomic pathways that drive ERMS pathogenesis, and to assess the extent to which a single histology and clinical risk group in this disease has a common molecular program, we conducted a high-resolution analysis of ERMS tumors.

PREDISPOSING FAMILIAL SYNDROMES

Although the majority of ERMS tumors arise spontaneously, children with predisposing familial syndromes, in which there are defects in the Ras, Hedgehog, and P53 pathways, are at higher risk for developing ERMS (Xia et al. 2002). It is not clear, however, what fraction of spontaneously occurring ERMS tumors are driven by these same pathways

NEUROFIBROMATOSIS & LI-FRAUMENI SYNDROME

Children with neurofibromatosis, caused by loss of Neurofibromin (*NF1),* a tumor suppressor responsible for converting active Ras-GTP to inactive Ras-GDP, have a twenty-fold increase in the likelihood of developing rhabdomyosarcomas (Sung et al. 2004). According to data from one study, five of 1,025 patients diagnosed with RMS had neurofibromatosis compared to a population prevalence of one in 3,000-4,000 (Ferrari et al. 2007; Sung et al. 2004). DNA sequence data also suggest the importance of Ras in ERMS development, as up to 50 percent of tumors have activating mutations in one of three Ras genes, *HRAS, NRAS* or *KRAS,* predominately the latter two (Schaaf et al. 2010); no Ras mutations were found in ARMS or pleomorphic RMS, an adult RMS variant (Martinelli et al. 2009; Stratton et al. 1989). Zebrafish and mouse models have confirmed that Ras activation, either by activating *KRAS* mutations or *NF1* deletion, can induce ERMS and pleomorphic RMS, although the mouse model requires *P53* inactivation to be penetrant (Langenau et al. 2007; Tsumura et al. 2006; Vogel et al. 1999). In mouse models, *P53* inactivation alone is enough to generate RMS at very low penetrance, a finding consistent with data from children with Li-Fraumeni syndrome, the inherited loss of the tumor suppressor *P53,* of whom ten

percent will develop RMS (Xia et al. 2002). DNA sequence data suggest that 5-30 percent of spontaneous RMS tumors have inactivation of *P53*; the largest study identified *P53* mutations in four of 36 RMS tumors (Chen et al. 2007; Diller et al. 1995; Felix et al. 1992; Taylor et al. 2000; Xia et al. 2002). Immunohistocheimcal studies would suggest that P53 inactivation might be more common in ERMS, as five (of ten) demonstrated high-level (three) or the absence of (two) P53 staining (Bridge et al. 2002).

GORLIN SYNDROME

Patients with Gorlin syndrome, who are heterozygous for loss of function mutations in the Hh negative regulator Patched (*PTCH1*), are prone to cancers including RMS (Tostar et al. 2005). Spontaneous ERMS tumors can also have loss of *PTCH1* or Suppressor of fused (*SU(FU)*), and very rare cases of amplification of the Hh-signaling downstream transcription factor *GLI1* have been identified in ARMS (Bridge et al. 2002; Bridge et al. 2000; Goldstein et al. 2006). Mouse models of Hh-induced cancers, including mice heterozygous for loss of function mutations in *PTCH1* or activating mutations affecting Smoothened (*SMO*) (Mao et al. 2006), a critical catalytic component of the Hh-signaling cascade, also develop ERMS among other tumor types including medulloblastoma and

basal cell carcinoma. These data suggest that increased Hh-signaling can induce ERMS, but it is not clear how common activation of the Hh-signaling cascade is in non-hereditary cases.

NON-FAMILIAL CANDIDATES

FGFR4 ACTIVATION

Recent studies have put forth another promising candidate in ERMS pathogenesis. High-level expression of the fibroblast growth factor receptor tyrosine kinase *FGFR4* is characteristic of rhabdomyosarcomas (Khan et al. 2001), and seven percent of ARMS and ERMS tumors have activating mutations in the kinase domain of *FGFR4* (Taylor et al. 2009). *FGFR4* is a direct target of the transcription factor PAX3, which drives essential aspects of the normal developmental program that generates skeletal muscle during embryogenesis (Lagha et al. 2008). *In vitro* and *in vivo* data, including RMS tumor xenografts with an RMS cell line, support the role of *FGFR4* in promoting growth and metastasis of RMS, likely through recruitment and activation of the STAT3 transcription factor to the cytoplasmic tail of the receptor (Dudka et al. 2010; Hart et al. 2000; Taylor et al. 2009).

IMPRINTING OF THE 11P15.5 LOCUS

Loss of heterozygosity, loss of imprinting, and paternal disomy of the 11p15.5 locus have previously been described in ERMS (Xia et al. 2002), all pointing to the importance of an imprinted gene in this region. The deletion of this locus suggests it harbors a tumor suppressor, and chromosome transfer studies carried out in ERMS using fragments of the locus suppressed proliferation, supporting this hypothesis (Xia et al. 2002). Of further interest, four cases of RMS have been reported in patients with Beckwith Wiedemann syndrome, which has rearrangement or loss of imprinting of the cytoband 11p15.5 (Xia et al. 2002). Several candidates of interest reside in this region, including H19, an untranslated mRNA maternally expressed during fetal development; the cell-cycle inhibitor CDKN1C ($p57^{KIP2}$); and Insulin-like growth factor (IGF2), which is largely hypothesized to be the target of the event (Xia et al. 2002). IGF2 is a fetal growth factor that regulates muscle cell differentiation and growth (Bridge et al. 2000), likely through activation of the PI3K/AKT-mTOR and MAPK/ERK pathways (De Giovanni et al. 2009). *In vivo* studies have supported IGF2 necessity for tumor growth in *PTCH1* loss of heterozygosity mice (De Giovanni et al. 2009; Hahn et al. 2000).

METHODS

SAMPLES

We obtained 26 frozen primary ERMS samples, eight from Children's Medical Center of Dallas (CMCD) and 18 from the Cooperative Human Tissue Network (CHTN), which banks tumors collected as part of the rhabdomyosarcoma clinical trials sponsored by the Children's Oncology Group (COG). The Soft Tissue Sarcoma Committee of COG and the University of Texas Southwestern Medical Center Investigational Review Board approved the use of these tumors. We obtained an additional 11 formalin-fixed paraffin-embedded intermediate-risk primary embryonal rhabdomyosarcomas from CMCD. There were no patients with known or suspected predisposing familial syndromes.

I also obtained clinical information, including: date of birth & diagnosis (or age at diagnosis), histological diagnosis, race, sex, tumor site, size and source of tissue sample, stage and group at diagnosis for risk determination, prior status (chemo/radiation), and patient status (alive, relapse, or death as applicable).

DNA ISOLATION

I isolated genomic DNA from 5 mg of frozen primary tumors. Samples were cut in half where possible, and roughly 5 mg of tissue was suspended in 200ul of SNET buffer (20mM pH 8 Tris, 400mM NaCl, 50mM pH 8 EDTA, 1% SDS) with 40ug of proteinase K. The samples were digested over night at 55 degrees with rotation. 4 ul of RNaseA was added to each sample and the samples were allowed to incubate at room temperature for 15 minutes. To each sample was added 100ul of TE and 300ul of Phenol:ChCl3. Following centrifugation at 13,000 rpm for 5 minutes, the bottom layer was discarded. After the addition of another 300 ul of chloroform and centrifugation at 13,000 rpm for 5 minutes, the top layer was transferred to a new tube were it was precipitated with 35uL of 3M pH 5.2 NaOAc and 1000ul of 100% EtOH at -20 degrees for 30 minutes. The samples were centrifuged at 13,000 rpm at 4* for 30 minutes. DNA pellet was washed in 70% EtOH, and then dried for 15 minutes prior to suspension in ddA/C water.

I assessed genomic DNA concentration and quality using a Nanodrop-1000 spectrophotemeter (Nanodrop); all samples met strict

cutoffs of 260/280 ≥ 1.8 and a 260/230 ≥ 1.9. Electrophoresis of 250 ng of genomic DNA on a 0.8 percent agarose gel confirmed the presence of a single band > 10 kb in size.

ROCHE NIMBLEGEN ARRAY COMPARATIVE GENOMIC HYBRIDIZATION (ACGH)

I sent 5 - 15 micrograms of genomic DNA to Roche NimbleGen (Reykjavik, Iceland) for aCGH using the 2.1 million probe platform (2.1 M), which utilizes genome-wide probe spacing of approximately every 1,110 bp, yielding an effective resolution of five to ten kilobases. We used pooled male reference genomic DNA provided by NimbleGen as comparitor DNA.

BIOINFORMATICS ANALYSIS

I imported normalized log2 probe signal values into Nexus Copy Number software (BioDiscovery) and segmented them using a five-probe call with three percent outlier removal and a significance threshold of 1E-08. We defined low-level gain and loss as log2 values of 0.2 and -0.18 respectively, and high-level amplification and deletion as ±0.5. We identified minimal common regions using the significant peaks feature,

using a STAC-p-value, and used visual inspection of probe plots to identify non-overlapping deletions that affected a single genomic locus. I also applied a candidate approach to identify amplifications and deletions of known oncogenes and tumors suppressors using public databases (Cancer Gene Census) and RMS candidate genes identified from the literature (De Giovanni et al. 2009). Regions of gain or loss contained within known copy number variable regions (CNVs) were discarded. To facilitate visualization of common regions of low-level loss or gain, I also aligned segmented Log2 values for all 26 tumors in Nimblescan (Roche).

GENOMIC IDENTIFICATION OF SIGNIFICANT TARGETS IN CANCER (GISTIC)

An independent, blinded analysis of our aCGH dataset was conducted using GISTIC as previously described by Rameen Beroukhim of the Broad Institute (Beroukhim et al. 2007).

GENE SET ENRICHMENT ANALYSIS (GSEA)

Using a published dataset of gene expression in RMS (Davicioni et al. 2009), I analyzed expression data from 60 ERMS and 37 translocation-positive ARMS tumors. GSEA analysis was carried out using a defined

gene-set (HSA05217_BASAL_CELL_CARCINOMA (Kanehisa et al. 2008), available from MSIG database), and using 1,000 phenotype permutations with a weighted enrichment statistic and a Singal2Noise Metric for ranking genes (Subramanian et al. 2005). Not all genes included in the gene-set were available in the data set for analysis. A p-value of <0.05 was defined as significant.

FLUORESCENT IN SITU HYBRIDIZATION (FISH)

FISH for probes against GLI1 (12q13.3, RP11-181L23), and its paracentromeric region (12p11.1,RP11-438D14), and GLI2 (2q14.2, RP11-57I19), and its paracentromeric region (2p11.2, RP11-269K22), (Signature Genomics) was carried out by the laboratory of Kathleen Wilson of UT Southwestern.

PCR AND SEQUENCING OF KNOWN MUTATIONS

Primers for Ras exons containing activating mutations, exon 2 and 3, were modified from (Schaaf et al. 2010); and primers for *FGFR4* exons containing activating mutations, exon 12 and exon 13, are as described in (Taylor et al. 2009). PCR and ExoSap conditions were modified from those previously described in (Taylor et al. 2009). Primer sequences and

PCR and ExoSap conditions are described in Table 1. Using reamplification and resequencing, I verified genes with suggested mutations. Garvin Chandler, of the Amatruda lab at UTSouthwestern, used TA cloning (into pCR®II-TOPO®, TOPO TA cloning Dual Promoter Kit, Invitrogen) of PCR product from patients with ambiguous *FGFR4* exon 13 sequence and sequencing of a minimum of six inserts to identify mutations.

RESULTS

To define the genomic programs that underlie ERMS pathogenesis, we used a newly available high-resolution array CGH platform that can identify copy number abnormalities with single gene resolution (Arlt et al. 2009). We obtained 26 ERMS tumor samples banked as part of treatment in Children's Oncology Group trials or in a local tumor bank at Children's Medical Center Dallas. The clinical characteristics of the patients are described in Table 2. All but two of these samples were from untreated patients and were diagnostic specimens from the primary tumor, one from a recurrence and another post-chemotherapy. Of these 26 samples, two were from children with clinically defined low-risk disease, as defined by current COG criteria (essentially no residual tumor after surgery), 21 were from intermediate-risk patients (microscopic or gross residual tumor after

surgery, absence of metastasis); two were from patients with high-risk (presence of metastasis); and one was from a patient with disease recurrence.

CYTOGENETIC ANALYSIS OF ERMS

We began our analysis by examining global chromosomal changes in the 26 ERMS tumors (Figure 1). The tumors were grossly aneuploid with many chromosomal abnormalities. The most common cytogenetic finding was polysomy 8 (>90 percent of samples), with many tumors having gained multiple copies, as has previously been described in ERMS (Bridge et al. 2002; Bridge et al. 2000; Gordon et al. 2001; Pandita et al. 1999; Williamson et al. 2010). We identified low-level gains of chromosomes 2, 11, 12, 13, 19, and 20 in 25-50 percent of tumors, and with the exception of chromosome 19 (which was identified as a more rare occurrence), gains of these chromosomes have been identified as occurring in 20–50 percent of cases (Bridge et al. 2002; Bridge et al. 2000; Gordon et al. 2001; Pandita et al. 1999; Williamson et al. 2010). We also identified low-level losses of chromosomes 6, 9, 10, 14, 15, 16 and 18 in 50-95 percent of patients. The literature in regards to these losses is less consistent, however several studies agree losses of chromosomes 6, 9,

10, 14, and 16 occur in 10-30 percent of cases (Bridge et al. 2002; Bridge et al. 2000; Gordon et al. 2001; Pandita et al. 1999; Williamson et al. 2010). The disparities between the frequency with which we observed these regions of decreased copy number and those of the literature likely reflects the sensitivity of our assay to genomic loss in heterogeneous tumors and our call threshold. The prevalence of common chromosomal changes, in particular gains of chromosome 8, suggests that there are genes within these regions that may contribute to ERMS pathogenesis.

AMPLIFICATION OF BCL2L1 AND LOSS OF PTEN WERE IDENTIFIED IN SINGLE TUMORS USING A CANDIDATE APPROACH

Using published databases of oncogenes and tumor suppressors, we sought well-defined small regions of high-level gain or loss in our dataset. Table 3 summarizes these findings, which include the identification of deletions affecting two well-known tumor suppressors; additional findings from this analysis are described below. In a single tumor, we identified deletion of a 50 kb portion of the tumor suppressor *PTEN* (Figure 2A), which has not previously been documented in ERMS. We also identified a single case of a focal amplification of a region containing the anti-apoptotic gene *BCL2L1* (Figure 2B), consistent with

several additional copies. *BCL2L1* was recently identified as a common target of amplification in a large aCGH dataset of cancer cell lines and human tumors, with supporting biological evidence that increased BCL2L1 expression is important for cancer cell survival (Beroukhim et al. 2010).

THE CDKN2A/B *LOCUS IS FREQUENTLY LOST IN ERMS TUMORS*

Recurrent regions of copy number abnormalities in the genomic DNA of tumors can identify genes that drive disease pathogenesis. We therefore focused on identifying recurrent regions of gain or loss using two software-based approaches, coupled with visual inspection of probe signals. Table 4 summarizes our findings.

Aberrant proliferation, often occurs through cell cycle dysregulation, decreased senescence, and impaired apoptosis, all functions of the most commonly mutated locus in cancer, *CDKN2A/B (CDKN2A: $p16^{INK4a}$/$p14^{ARF}$ and CDKN2B: $p15^{INK4B}$)* (Beroukhim et al. 2010; Kim and Sharpless 2006). $p16^{INK4a}$ prevents G1 to S transition via inhibition of CDK4/6, as does $p15^{INK4B}$, and accumulates with aging and under stress to promote senescence; its alternative transcript, $p14^{ARF}$, stabilizes P53 (Kim and Sharpless 2006).

We identified deletions of *CDKN2A/B* in 25 percent (6/26) of tumors (Figure 3). The level of loss in these patients was suggestive of homozygous deletion (Log2 range: -0.7 to -2.0), and as *CDKN2A/B* were the only genes affected by several of these deletions, we identified this locus as the target of the deletions. Moreover, 25/26 patients showed an apparent heterozygous loss (Log2 <-0.18) of 9p/9, the chromosome arm/chromosome on which *CDKN2A/B* resides, suggesting that additional tumors may have reduced CDKN2A/B function, which may be further decreased by a second allele that carries small mutations not detected by aCGH.

FGFR4 IS ACTIVATED THROUGH PREFERENTIAL AMPLIFICATION OF MUTANT ALLELES, AND ALSO BY MUTATION WITHOUT AMPLIFICATION IN ERMS

Receptor tyrosine kinases, often growth factor receptors, are common targets of activation in human cancer and represent potential targets in effective antineoplastic therapy (Imai and Takaoka 2006; Kim and Sharpless 2006; Zwick et al. 2002). We identified amplification of Fibroblast growth factor receptor 4 (*FGFR4)* in 15 percent (4/26) of patients, at levels suggestive of multiple additional copies (Log2 range: 0.7

to 1.1) (Figure 4). The recent identification of activating mutations affecting the *FGFR4* tyrosine kinase domain (N535D/K and V550E/L), and biological studies demonstrating the necessity of FGFR4 for proliferation of RMS xenografts (Taylor et al. 2009), led us to analyze our samples for these mutations. Mutations at V550 are thought to alter the ATP binding site (Mohammadi et al. 1998; Torkamani and Schork 2008), while those at N535 are thought to abolish hydrogen bonds that regulate receptor autophosphorylation and/or conformation (Chen et al. 2007). We identified activating mutations in all four *FGFR4* amplifications (1 N535D, 2 V550L, and 1 V550M), and in an additional patient who did not have amplification of the locus (V550L) (Table 5). These data indicate that genomic changes affecting *FGFR4* occur in five of 26 patient samples, with at least two different modes of possible activation, and strongly support the importance of *FGFR4* in ERMS pathogenesis.

THE HEDGEHOG PATHWAY MAY BE ACTIVATED IN ALL ERMS

Cancer cells can co-opt developmental pathways that regulate cell division, patterning, and differentiation of tissues during embryogenesis to promote essential aspects of the malignant phenotype including proliferation and insensitivity to anti-growth signals (Jiang and Hui 2008;

Münsterberg et al. 1995). Hedgehog (Hh) is a developmental pathway that patterns many developing tissues and organs, including muscle development (Jiang and Hui 2008; Münsterberg et al. 1995). Defects in Hh-signaling are common in human cancers, classically basal cell carcinoma and medulloblastoma (Gailani et al. 1996; Johnson et al. 1996; Lam et al. 1999; Taipale and Beachy 2001; Wolter et al. 1997; Xie et al. 1997). We identified very low-level gains (Log2 >0.2) of two transcription factors that are essential mediators of Hh-signaling, *GLI1* (14 tumors) and *GLI2* (24 tumors), with more than half of tumors demonstrating gains in both (Figure 5, Figure 6). As many of the gains were low-level and extended over larger regions, we sought to confirm our finding by means of an independent blinded analysis utilizing an alternative approach, genomic identification of significant targets in cancer (GISTIC) (Beroukhim et al. 2007). GISTIC identified a region containing *GLI2* (2q14.2) as commonly and significantly gained (q-value, 8.69E-08) (Figure 5B). GISTIC also identified the region 12q13.3 as commonly and significantly gained with a peak q-value of 5.23-07; *GLI1* is adjacent to this region and also appears significantly gained (Figure 5B). FISH confirmed gains of *GLI1* but not *GLI2* (Figure 7).

To further examine whether the low level GLI amplifications were significant, we hypothesized that the observed gains in downstream Hedgehog effectors might produce a gene expression signature that reflected pathway activation. We analyzed published expression data (Davicioni et al. 2009) from 60 ERMS and 37 translocation-positive ARMS using gene set enrichment analysis (GSEA), comparing ERMS to ARMS. Remarkably, a gene set initially defined for basal cell carcinoma (Kanehisa et al. 2008), a cancer classically defined as having Hh activation, was significantly enriched ($p<0.001$) in ERMS (Figure 8). Amongst the genes contributing the most to this enrichment were *GLI1, GLI2,* another Hedgehog transcription factor *GLI3*, and the Hh-pathway negative regulator and GLI target *PTCH1*. These were the only Hedgehog pathway members included and analyzed in the gene-set (aside from SHH which did not contribute to enrichment), and a comparison of expression levels of these genes revealed an increase in the average expression of GLI1, GLI2, GLI3 and PTCH1 in ERMS, while SHH remained unchanged. Other key contributors to this core enrichment include several members of the WNT signaling developmental pathway that are over-expressed in basal cell carcinoma and are thought to be downstream of the GLI transcription factors in WNT regulation: WNT5a, WNT11, and WNT 10b (Mullor et al. 2001). This finding is consistent with Hh-pathway activation at the level of

GLI transcription factors, and potentially their subsequent activation of other pathways important in malignancies.

NF1 ***DELETION IS AN ALTERNATIVE METHOD OF RAS PATHWAY ACTIVATION IN ERMS***

Ras pathway activation is thought to occur in approximately one-third of human cancers by activating mutation alone, and is responsible for increased proliferation and decreased differentiation of tumor cells (Scalzone et al. 2009; Schaaf et al. 2010). Loss of function mutations in the Ras-GAP *NF1* locus also result in Ras activation. *NF1* enhances the GTPase activity of Ras, promoting Ras inactivation (Scalzone et al. 2009). We identified small, in some cases intragenic non-overlapping deletions of the *NF1* locus, which spans a 350 kb region, in 15 percent (4/26) of tumors (Figure 9). One deletion eliminated the majority of the gene and others deleted 50-100 kb segments including several exons. *NF1* was the only gene deleted in all four samples, with levels of loss suggestive of homozygous deletion (Log2 values: -0.7 to -1.0). An additional five patients showed an apparent heterozygous loss of *NF1*, three of which were focal (Figure 10). Heterozygous deletions affecting *NF1* may reflect a distinct mechanism of bi-allelic inactivation, such as deletion of one

allele and point mutation of the other as has been described in glioblastoma (Cancer Genome Atlas Research Network 2008), ovarian cancer (Sangha et al. 2008), and leukemia (Balgobind et al. 2008).

We hypothesized that a majority of ERMS tumors might have Ras activation by *NF1* deletion and by activating Ras mutations, which have previously been described in ERMS (Martinelli et al. 2009; Schaaf et al. 2010). We therefore sequenced *HRAS, KRAS,* and *NRAS* for known activating mutations and found 12 mutations in 42 percent (11/26) of our patient samples (Table 6). One patient demonstrated activating mutations in both *NRAS* and *HRAS*. None of the patients with Ras mutations displayed homozygous deletion of *NF1*, suggesting that tumors require Ras activation by either *NF1* loss or Ras activation, but not typically both. Together, 58 percent (15/26) tumors in our dataset had activation of the Ras pathway either by *NF1* deletion or activating point mutations affecting one of the Ras genes.

DISCUSSION

COMMON GENOMIC PROGRAMS DRIVE PATHOGENESIS OF INTERMEDIATE RISK ERMS PATIENTS

Identification of common programs underlying ERMS pathogenesis is important to better understand what drives tumor formation. By understanding these mechanisms, we can develop improved mouse models that more closely model human ERMS and improved approaches to patient therapy. Our analysis identified amplifications and deletions of loci not previously known to be involved in ERMS pathogenesis, and the very high resolution of this platform allowed us to assign with confidence the target genes affected by the copy number abnormalities. Our data suggest that there are common genomic programs that underlie pathogenesis in intermediate-risk ERMS patients, including inactivation of *CDKN2A/B* and activation of the *FGFR4* receptor tyrosine kinase, Ras, and Hedgehog pathways. A summary of patient findings is given in Table 7.

CDKN2A/B in ERMS likely promotes increased proliferation and replicative potential of tumors cells, decreased senescence, and impaired apoptosis

CDKN2A (p16^{INK4a}/p14^{ARF}) and *CDKN2B* (*p15^{INK4B}*) are among the most commonly mutated genes in human cancer, and a recent large-scale study (3,131 cell lines and primary tumors containing 26 histologies) identified their focal deletion in 14 percent of samples (Beroukhim et al. 2010). Both p16^{INK4a} and p15^{INK4B} inhibit G1 to S cell cycle transition through abrogation of CDK4/6 activation by cyclin D; this results in hypophosphorylated RB, which sequesters the E2F transcription factor (Kim and Sharpless 2006). Additionally, p16^{INK4a} also promotes senescence and limits replicative potential of stem cells following its accumulation during aging and/or exposure to genotoxic stress (Kim and Sharpless 2006). p14^{ARF} stabilizes P53 by sequestering its binding partner MDM2, promoting P53 accumulation and also resulting in cellular senescence, or in the case of irreparable genomic damage, apoptosis (Kim and Sharpless 2006). We found focal deletions of *CDKN2A/B* in approximately 23 percent (6/26) of ERMS samples, consistent with prior work (Iolascon et al. 1996). Additional studies in primary RMS tumors have described heterozygous deletion of *CDKN2A* in 12 to 20 percent of samples (Chen et al. 2007; Williamson et al. 2010). It can be difficult to

distinguish heterozygous from homozygous deletion using aCGH, as the fraction of tumor cells versus surrounding stromal cells is often not documented. Our data suggest that as in other cancers, focal deletion of *CDKN2A/B* ($p16^{iNK4a}$, $p14^{ARF}$, $p15^{iNK4B}$) in ERMS promotes increased proliferation and replicative potential of tumor cells, decreased senescence, and impaired apoptosis.

Maintained FGFR4 activation is necessary for tumor survival

We also identified activation of the receptor tyrosine kinase gene *FGFR4* in 20 percent (5/26) of ERMS samples, most commonly through amplification of a mutationally activated allele. *FGFR4* is a direct target of the transcription factor PAX3 and controls entry of embryogenic muscle progenitor cells into the myogenic program (Lagha et al. 2008). Activation of FGFR4, and family members FGFR1, FGFR2, and FGFR3, through amplification, over-expression, and mutation has previously been described in several cancers (Cappellen et al. 1999; Ding et al. 2008; Kunii et al. 2008; Pollock et al. 2007; Rand et al. 2005; Reis-Filho et al. 2006; Sahadevan et al. 2007).

In RMS, there are reports of *FGFR1* amplification, one case in pleomorphic RMS (Goldstein et al. 2006) and three cases each in ERMS (of 51) and translocation-negative ARMS (of 27) (Williamson et al. 2010). We did not observe *FGFR1* amplification likely due to *FGFR1's* position on chromosome 8, for which we observed copy number gains across the entire chromosome evenly split between low-copy gains (log2 values of 0.2-0.5) and high-copy level gains (log2 values of 0.5-1.0), suggestive of multiple additional copies of chromosome 8.

In prostate cancer, over-expression of FGFR4 correlates with increased stage and poor prognosis, and *in vitro* studies suggest FGFR4 is required for prostate cancer cell survival (Sahadevan et al. 2007). In RMS, FGFR4 is broadly expressed and expression distinguishes RMS tumors from other histologically similar small round blue cell tumors (Khan et al. 2001). Amplification of the *FGFR4* gene has not been described in RMS, but *in vitro* and some *in vivo* data suggest that activation of FGFR4 signaling, mediated by STAT3, promotes proliferation and metastasis of RMS tumors (Taylor et al. 2009). Functionally *FGFR4* activating mutations in RMS cell lines appear significantly more potent than wild-type FGFR4, but mouse xenografts have demonstrated that expression of FGFR4, wild-type or mutant, is necessary for maintenance of the primitive tumor

phenotype and for proliferation of tumor cells (Taylor et al. 2009). Our data support the idea that FGFR4 is an excellent candidate for the application of a small molecule inhibitor or biological inhibitor to improve treatment of ERMS.

Hedgehog promotes ERMS tumorigenesis

Many studies have proposed that Hedgehog pathway activation contributes to ERMS pathogenesis. Several studies identified loss of heterozygosity (8-35 percent of patients) and deletions (33 percent of patients) of a large region containing *PTCH1* among many other genes *(*cytoband 9q22) (Tostar et al. 2005); however, *PTCH1*-specific mutations have not been detected in spontaneous RMS tumors (14 sequenced samples) (Calzada-Wack et al. 2002). This finding is surprising, as other tumors associated with Hh activation have inactivating mutations in *PTCH1*, 30-40 percent of basal cell carcinomas and 20 percent of medulloblastomas (Gailani et al. 1996; Johnson et al. 1996; Lam et al. 1999; Wolter et al. 1997; Xie et al. 1997). Mouse models heterozygous for *PTCH1* loss-of-function mutations or activating *SMO* mutations (Hahn et al. 1998; Mao et al. 2006) develop ERMS at low frequency, as do those with *SU(FU)* loss of function in a *P53* null background (Lee et al. 2007),

further supporting the role of Hedgehog in ERMS pathogenesis. We did not identify regions of *SMO* amplification or *PTCH1* deletion, but we did observe remarkably frequent low-level gains of *GLI1* and *GLI2,* the transcription factors responsible for downstream Hedgehog signaling, and an ERMS-specific gene expression signature that supports activation of the pathway in this tumor. Previous studies identified gains of cytoband 12q13-15 in up to 50 percent of RMS tumors, but as this region contained multiple other oncogenes including *CDK4*, *MDM2*, and *GLI1*, the target of the amplifications was unclear (Bridge et al. 2002; Bridge et al. 2000; Williamson et al. 2010). In one study, the observed ARMS case (one of seven) verified the increased copy number of *CDK4* and *SAS* (10-12 copies) and *GLI1* (7-8 copies) using FISH (Goldstein et al. 2006). Our data suggest that the target of the 12q13-15 gain in ERMS is *GLI1*, and that *GLI2* is also gained in a majority of RMS tumors. GLI1 and GLI2 can inhibit differentiation of mouse-model rhabdomyosarcoma cell lines by preventing the formation of a MYOD/E12/DNA binding complex necessary for transcriptional activation of MYOD targets (Gerber et al. 2007). These findings suggest that amplification of *GLI1* and *GLI2* contribute to ERMS pathogenesis in part by inhibiting MYOD-induced differentiation, and likely through other targets as well. Additional downstream targets of GLI transcription factors, such as Insulin like growth factor 2 (*IGF2*) and

members of the WNT pathway, may also be important in ERMS pathogenesis. IGF2, a regulator of muscle cell differentiation and growth, is often over-expressed in RMS (Xia et al. 2002) and is required for the generation of rhabdomyosarcomas in the *PTCH1* mouse model (Hahn et al. 2000). The WNT pathway has not been extensively studied in RMS (Bouron-Dal Soglio et al. 2009). Basal cell carcinoma is characterized by increased expression of members of the WNT signaling developmental pathway including, WNT5a, WNT11, and WNT 10b (Hoseong Yang et al. 2008; Mullor et al. 2001), and in addition to the Hh-pathway genes the WNTs are among the key contributors to enrichment of the GSEA basal cell carcinoma gene set in ERMS we identified. Our data suggests Hedgehog pathway activation in ERMS occurs at the level of GLI transcription factors, suggesting that this disease may be resistant to currently available inhibitors of Hh activity, which act upstream of the GLI transcription factors on the target SMOOTHENED (Jiang and Hui 2008).

Ras activation occurs in a majority of ERMS patients

Patients with neurofibromatosis have increased Ras pathway activity and are at an increased risk of developing ERMS. Homozygous inactivation of *NF1* has been described in other cancers including

glioblastoma (Cancer Genome Atlas Research Network 2008), ovarian cancer (Sangha et al. 2008), and in a subset of leukemias (Balgobind et al. 2008), but to the best of our knowledge, has not previously been reported in spontaneous cases of RMS. In glioblastoma, homozygous deletion of *NF1* and biallelic inactivation of *NF1* by missense or nonsense mutations in both alleles occurred with equal frequencies, in three percent of patients (Cancer Genome Atlas Research Network 2008). The findings in ovarian cancer were similar; as seven percent of patients had homozygous deletion of *NF1*, while an additional seven percent had heterozygous deletion of *NF1* and mutation of the remaining allele (Sangha et al. 2008). Finally, bi-allelic inactivation of *NF1* via deletion and mutation was observed in 2 percent of T-cell acute lymphocytic leukemias and MLL-translocation-positive mixed lineage leukemias (Balgobind et al. 2008). Our finding of homozygous (15 percent) and heterozygous (10 percent) micro-deletions affecting *NF1* suggests that *NF1* inactivation is common in spontaneous cases of ERMS, and that additional tumors have inactivated *NF1* by mechanisms not detected by aCGH, such as point mutations or micro-deletions. Based on these findings, we conclude that a majority of ERMS tumors have activation of the Ras pathway either by direct activation of Ras by mutation or by *NF1* loss. Genome sequence data of ERMS tumors will address this possibility.

THERAPEUTIC IMPLICATIONS OF A GENOMIC SIGNATURE FOR INTERMEDIATE RISK ERMS

A central focus of current cancer research is the identification of genetically defined subsets of patients that are predicted to respond to specific inhibitory pharmaceuticals that target the mutant pathways. Our data, together with those of others, have important implications for delivering effective targeted therapy.

MEK inhibitors are currently in clinical trials

Inhibitors of components of the MAP kinase cascade downstream of Ras signaling are in clinical trials, including RAF and MEK inhibitors (Flaherty et al. 2010; Lorusso et al. 2010; Solit et al. 2006; Tawbi and Nimmagadda 2009). Our data, and those from other work cited above, support Ras pathway activation in ERMS and suggest that preclinical investigation of Ras pathway inhibitors is warranted. Perhaps these inhibitors can be tested using improved genetically engineered mouse models, as described below, in conjunction with more traditional models of human cancers, including tumor xenografts.

FGFR4 is an excellent candidate for the development of small molecule inhibitors in ERMS treatment

Similarly, our identification of *FGFR4* activation in 20 percent of ERMS patients, and evidence from previously published data (Taylor et al. 2009), supports the idea that RMS patients may benefit from treatment with FGFR4 antagonists, either antibodies or small molecule inhibitors of tyrosine kinase activity (TKIs). Whether inhibitory antibodies or TKIs will be more effective is not clear, but studies carried out in EGFR, a tyrosine kinase often amplified and/or mutated in cancers, may be informative (Imai and Takaoka 2006; Storlazzi et al. 2005). Both preclinical *in vitro* and *in vivo* data support the use of TKIs (gefitinib or erlotinib) as opposed to mAbs (cetuximab) in the treatment of non-small cell lung cancer (NSCLC), which is known to harbor activating mutations of EGFR (Gazdar and Minna 2008; Imai and Takaoka 2006; Liu et al. 2007). By comparison, colon cancer patients, whose tumors are less likely to have an activating EGFR mutation, respond more favorably to cetuximab; patient response correlates with DNA copy number (Gazdar and Minna 2008; Imai and Takaoka 2006; Liu et al. 2007). Given that we identified only mutant, amplified *FGFR4*, TKIs may be more effective in ERMS, but this will require appropriate agents and preclinical testing. Moreover, because many RMS tumors express *FGFR4* and do not appear to carry activating

mutations, other strategies including inhibitory antibodies may be effective broadly in this disease.

Hedgehog pathway inhibitors currently in trial may not be effective in ERMS patients

Extensive efforts are also underway to develop Hh-pathway inhibitors. Inhibitors of the Hedgehog pathway currently in clinical trial all act at the level of SMOOTHENED (GDC-0449, IPI926, XL139, LDE225, and PF-04449913, clinicaltrials.gov), which is upstream of the GLI transcription factors. It will therefore be important to determine whether patients with gains of GLI will respond to use of these inhibitors. Preliminary evidence from *in vitro, in vivo,* and clinical data suggests they will not. Mouse models have demonstrated that RMS tumors arising from mechanisms at or downstream of *SMO* are resistant to the SMO antagonist cyclopamine (Lee et al. 2007; Taipale et al. 2000). As RMS tumors with CMV driven GLI2 expression are also immune to SMO antagonists (Taipale et al. 2000), it is likely that patients with amplification of GLI transcription factors will not respond to these inhibitors. However, rather than assess the sensitivity of ERMS to Hedgehog inhibitors using cells with virally-driven GLI expression, the identification and use of ERMS

cell lines with an aCGH profile similar to those we describe could provide a more clinically relevant model for testing of potential inhibitors.

MOUSE MODELS FOR THE ASSESSMENT OF NOVEL ERMS THERAPEUTICS

At present there are no mouse models of rhabdomyosarcoma that utilize combinations of the genetic lesions identified here, although many models make use of the individual lesions we and others have identified. Genetically engineered mouse models with mutations in each of the genes described here have already been generated, with the exception of gain of GLI function. Mice with combinations of the genetic lesions described here can therefore be generated using existing reagents. Whether these combinations will develop disease that more closely resembles that of human ERMS, and whether such mice will be improved models for testing strategies for therapeutic interventions, remains to be seen.

Table 1: Primers, PCR, Exosap, and Sequencing Conditions

Primers	
FGFR4 Exon 12 Forward Primer *	GATTCAGCCCTAGACCTACG
FGFR4 Exon 12 Reverse Primer	CACTCCACGATCACGTAC
FGFR4 Exon 13 Forward Primer *	CAACCTGCTTGGTGTCTG
FGFR4 Exon 13 Reverse Primer	GGAAAGCGTGAATGCCTG
HRAS Exon 2 Forward Primer *^	GAGACCCTGTAGGAGGACCC
HRAS Exon 2 Reverse Primer	TCTAGAGGAAGCAGGAGACAGG
HRAS Exon 3 Forward Primer *^	CTATAGAGGTGAGCCTGGCG
HRAS Exon 3 Reverse Primer ^	GATCTGCTCCCTGAGAGGTG
NRAS Exon 2 Forward Primer *	TGAGGCCGATATTAATCC
NRAS Exon 2 Reverse Primer ^	GAGAGACAGGATCAGGTCAG
NRAS Exon 3 Forward Primer	GGCAGAAATGGGCTTGAATA
NRAS Exon 3 Reverse Primer *	GGTAACCTCATTTCCCCATAAAG
KRAS Exon 2 Forward Primer *	TTAACCTTATGTGTGACATGTTCTAA
KRAS Exon 2 Reverse Primer	AGAATGGTCCTGCACCAGTAA
KRAS Exon 3 Forward Primer *	TGCACTGTAATAATCCAGACTGTG
KRAS Exon 3 Reverse Primer	TGCATGGCATTAGCAAAGAC

* Primers different than previously published primers
^ Sequencing Primer

PCR Mix (15ul rxn)	
150ug DNA (template)	X
2uM Primers: Forward & Reverse	1.5 ul
60% glycerol	2 ul
Taq Buffer (10x)	1.5 ul
dNTPs (2mM)	1.5 ul
MgCl2 (50mM)	0.6 ul
Taq enzyme	0.15 ul
H2O	to 15 ul

PCR Conditions		
Initial Denature	94*, 3 min	
Denature	94*, 15 sec.	30 sec, 34 cycles (Except H3, N3: 39 cycles)
Anneal	63.5* (Except H2, H3: 66*), 30 sec	
Extension	72*, 45 sec.	
Final Extension	72*, 10 min	
Hold	16*, hold	

ExoSap Mix	
Exo sap enzyme (USB)	2 ul
PCR product (template)	5 ul

Exo Sap Conditions
1 hr, 37*
20 min, 72*

Sequencing	
ExoSap reaction	7 ul
Sequencing primer (1uM)	6 ul

Table 2: Embryonal rhabdomyosarcoma patient demographics

Tumor ID	Sex	Age	Location	Stage	Group	Risk	Status
1	F	4	Orbit	1		Low	Alive
2	F	4	Posterior nasal septum	1	2	Low	Alive
3	F	5	Nasal cavity & sinus	2(T1,N0)	3	Int	Alive
4	M	12	Nasopharynx	2 (T1,N0)	3	Int	Alive
5	M	5	Middle Ear	2(T2,N0)	3	Int	Alive
6	M	6	Nasopharynx	2(T2,N0)	3	Int	Dead
7	M	4	Retroperitoneum	3 (T1,N0)	3	Int	Alive
8	M	1	Bladder, pelvic mass	3 (T1,N0)	3	Int	Progression
9	F	4	Retroperitoneum	3 (T2,N0)	3	Int	Dead
10	F	5	Retropertioneum	3 (T2,N0)	3	Int	Dead
11	M	12	Prostate	3 (T2,N0)	3	Int	Alive
12	F	2	Middle Ear	3 (T2,N0)	3	Int	Dead
13	M	4	Bladder	3 (T2,N0)	3	Int	Alive
14	F	4	Larynx w/ PM extension	3 (T2,N0)	3	Int	Dead
15	F	4	Retroperitoneum	3 (T2,N0)	3	Int	Alive
16	M	3	Bladder	3 (T2,N0)	3	Int	Alive
17	F	1	Nasopharynx	3 (T2,N0)	3	Int	Dead
18	M	9	Nasopharynx	3 (T2,N0)	3	Int	Dead
19	F	6	Pelvic, indeterminant	3 (T2,N0)	3	Int	Progression
20	M	6	Cheek w/ PM extension	3 (T2,N0)	3	Int	Progression
21	M	5	Middle ear & Nasopharynx	3	3	Int	Alive
22	M	7	Retroperitoneum	3	3	Int	Alive
23	M	4	Nasopharynx	3	3	Int	Alive
24	M	7	Peripharyngeal, head/neck/face	3		High	Alive
25	F	5	Pelvic Mass	4		High	Alive
26	F	6(8)	Omentum, Bladder	4, recurrent		High	Dead

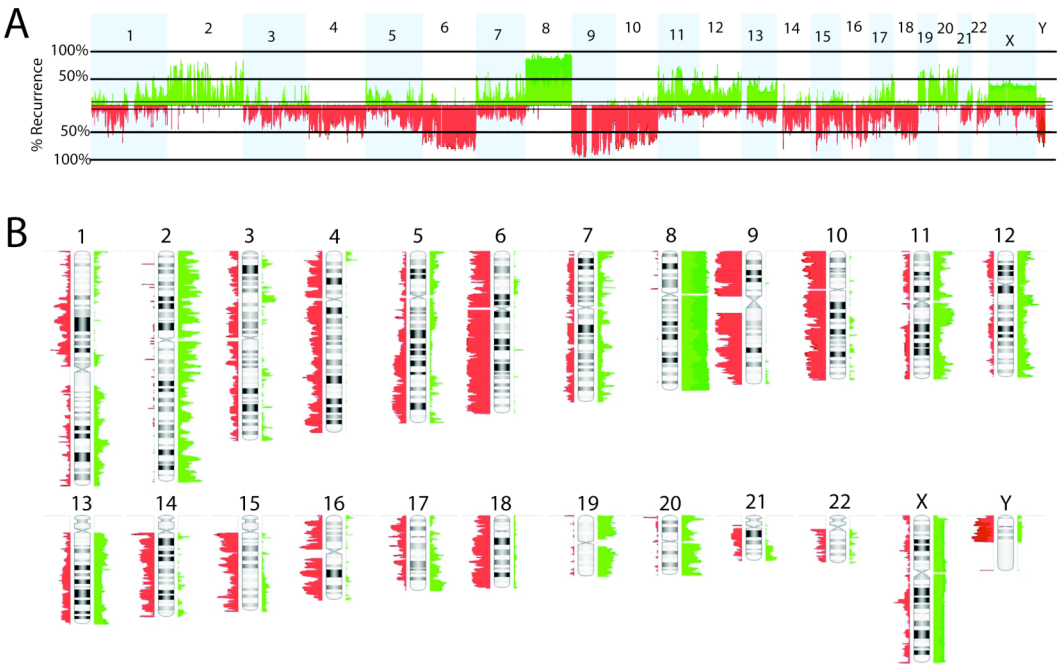

Figure 1: Summary of the copy number abnormalities in 26 ERMS tumors.

(A&B) Two different representations of the frequency of gains (green) or losses (red) detected at particular chromosomal locations across the genome are shown. Color intensity indicates level of gain/loss, darker (higher) and lighter (lower). aCGH data are normalized to male reference genomic DNA.

Table 3: Copy number abnormalities affecting oncogenes, tumor suppressors, and RMS candidates

Gene	Cytoband Band Location	Function/ Finding	Event	Size and # of event(s)	Number of genes in smallest region
ATM	11q22.3	Tumor supressor	Loss	1 small region	3
BCLXL/ BCL2L1	20q11.21	Anti-Apoptotic	Gain	1 small region	5
BIN1	2q14.3	RMS, low expression. High levels of expression= good outcome	Gain	4 small region	1
CD74	5q32	Translocation partner	Gain	1 microamplification	4
CDKN2A/B	9p21.3	Cell cycle, Tumor supressor	Loss	Common region of loss	1
FAM123B/ WTX	Xq11.1	Tumor supressor involved in Wilm's tumor	Gain	2 arm level, 3 microamplifications	2
FOXO4 / MLLT7	Xq13.1	Translocation partner in cancer	Gain	8 large, 1 small region	5
FGFR4		Overexpressed in RMS	Gain	Common region of gain	1
GLI2	2q14.2	Hedgehog pathway activator	Gain	Common region of gain	1
GPC3	Xq26.1	Overexpressed in RMS	Gain	4 large regions, 1 microamplification	5
HDGFRP3	15q25.2	High levels of expression= poor outcome	Loss	1 small region loss	4
HRAS	11p15.5	RAS pathway activator	Gain	4 large regions, 1 microamplification	15
IGFBP2, 5	2q35	Up in translocation negative ARMS- (IGFBP5 is up in poorly differentiated RMS, and overexpressed in RMS)	Gain	1 microamplification, 1 med region, and 1 large region	2
IRF4	6p25-p23	Translocation partner in cancer	Loss	2 small regions	2
KDM5C/ JARID1C	Xp11.22-p11.21	Chromatin remodeling, Transcription regulation	Gain	6 large regions, 1 small region	2
LHFP	13q12	Translocation partner in cancer	Gain & Loss	1 large region gain, 1 microdeletion	2
LMO1	11p15	Translocation partner in cancer	Gain	1 large region, 1 microamplification	3
LYL1	19p13.2-p13.1	Translocation partner in cancer	Gain	1 large region, 1 microamplification	3
MAPKAPK3	3p21.31	High levels of expression= good outcome	Gain	1 large region	24
MARS	12q13.3	High levels of expression= poor outcome	Gain	4 large regions	13
MYF5	12q21.31	Down in translocation positive ARMS; mucle differentiation factor	Loss	1 microdeletion	10
NF1	17q11.2	Tumor supressor	Loss	Common region of loss	1
NFIB	9p24.1	Translocation partner in cancer	Loss	1 microdeletion	3
NSD1	5q35	Translocation partner in cancer	Loss	1 small region	21
OBSL1	2q35	High levels of expression= good outcome	Gain	5 small regions	10
PAX8	2q12-q14	Translocation partner in cancer	Gain	3 small regions	3
PCSK7	11q23.3	Translocation partner in cancer	Gain	2 small, 1 large region	3
PER1	17p13.1-17p12	Translocation partner in cancer	Loss	1 small region	3
PIM1	6p21.2	Translocation partner in cancer	Loss	1 small region	5
PTEN	10q23.3	Tumor supressor	Loss	1 large region, 1 microdeletion	1
PTMA	2q37.1	Up in translocation negative ARMS	Gain	1 small region	1 gene, 1 miR
SMO	7q31-q32	Hedgehog pathway activator	Gain	1 large region	15
SPRY3	Xq28	Antagonist of FGF	Loss	1 small region	2

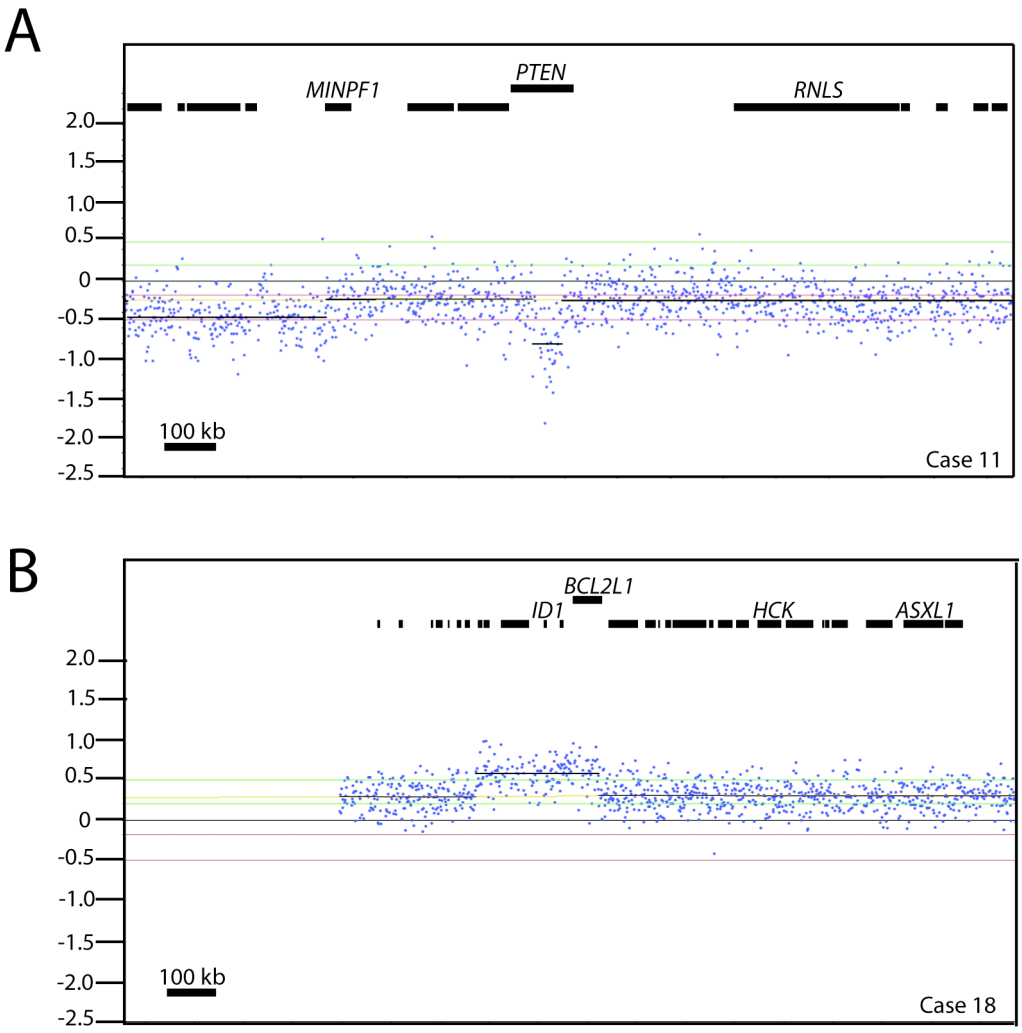

Figure 2: Copy number loss of the *PTEN* tumor suppressor and copy number gain of the antiapoptotic locus *BCL2L1*.

Black bars above represent genes in the region. Not all genes in the region are labeled. **(A)** Focal deletion of *PTEN* seen in one case (case 11). **(B)** Gain of a region containing *BCL2L1* and 6 other genes (case 18). Blue dots represent signals from individual probes, and black line segments represent averaged probe signals across a region.

Table 4: Focal regions of loss and gain in embryonal rhabdomyosarcoma

Cytoband	Size of smallest region (kb)	Event	Frequency (%)	STAC P-value	Amplitude: Log_2 Range	Genes
2p21	130.65	Gain	15	0.01	0.5 to 0.7	TTC7A
2q35	250.93	Gain	15	0.038	0.5 to 0.7	TNS1
2q14.2	941.36	Gain	92+	^	0.3 to 0.6	GLI2
2q36.1	306.66	Gain	8	^	0.5 to 0.6	MOGAT1
5q35.2 - q35.3	165.40	Gain	15	0.013	0.7 to 1.1	FGFR4
11p11.2	140.29	Gain	19	0.01	0.5 to 0.9	CREB3L1, DGKZ
11q24.2	35.49	Gain	19	^	0.5 to 1.0	ROBO3, ROBO4
12q13.3	48.15	Gain	53+	^	.2 to .65	IHBC, INHBE, GLI1, ARGHAP9, MARS, DDIT3, MBD6, DCTN2, KIF5A, PIP4K2C, DTX3, GEFT, SLC26A10, B4GALNT1
12q13.3	124.12	Gain	23	0.008	0.6 to 0.8	LRP1, NXPH44, SHMT2, NDUFA412, miR1228
1p36.23	14.30	Loss	8	^	-0.6 to -0.8	RERE
1q32.1	95.90	Loss	8	^	-0.5 to -0.6	PPP1R12B
3p14.2	1,077.83	Loss	8	^	-0.6 to -0.8	PTPRG, FHIT
4q35.1-35.2	929.88	Loss	8	^	-0.7 to -0.8	F11, ANKRD37, UFSP2, C4orf47, CCDC110, PDLIM3, SORBS2, TLR3, FAM149A, CYP4V2, KLKB1
9p21.3	2.38	Loss	23	*	-0.7 to -2.0	CDKN2A/B
17q11.2	57.07	Loss	15	*	-0.7 to -1.0	NF1
22q13.31	197.92	Loss	8	^	-0.5 to -0.7	ATXN10

+ Frequency of low level gain and loss of the region containing GLI1 and GLI2
^ Indicates p-values that are not available due to surrounding regions of gain or loss
* Indicates p-values that are not available due to failure of the software to detect non-overlapping deletions

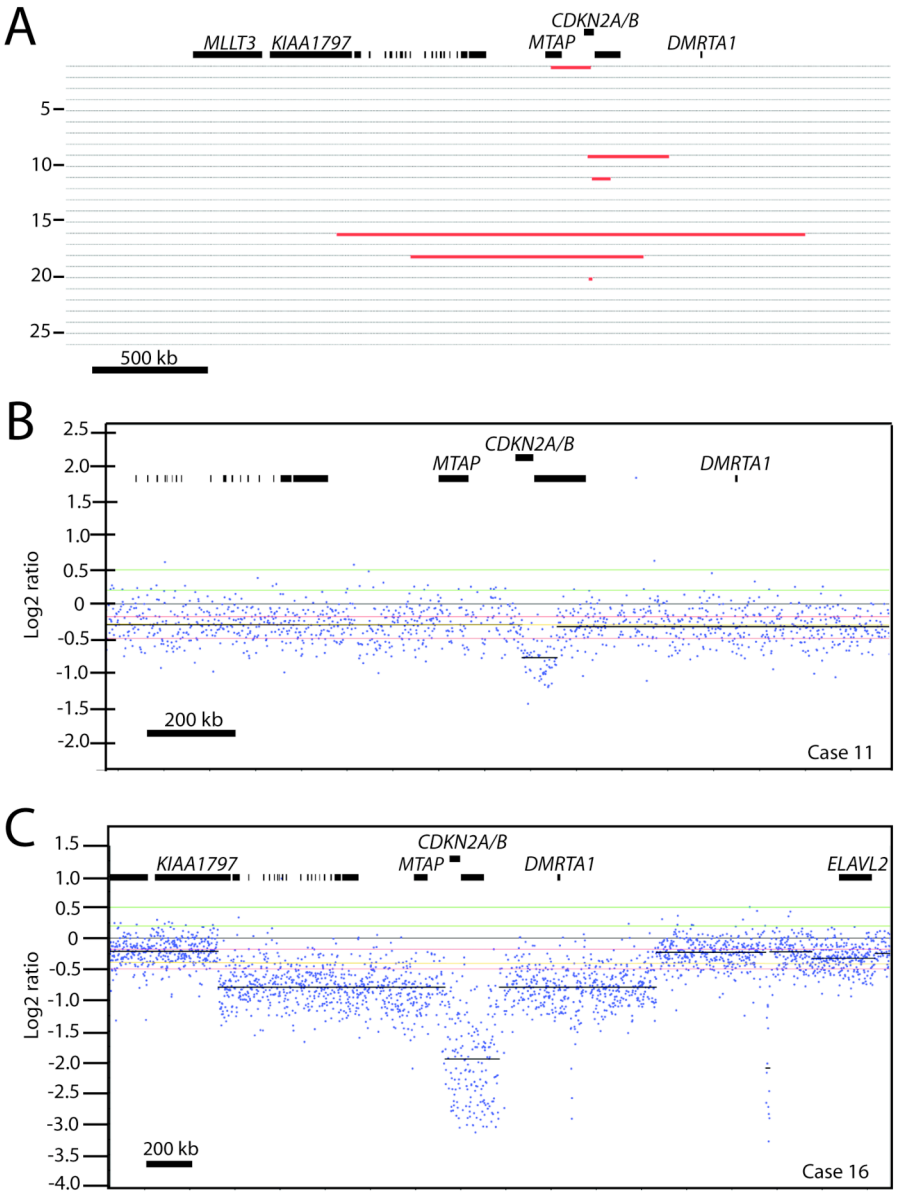

Figure 3: CDKN2A and B are deleted in ERMS.

Black bars above represent genes in the region (9p21.1-9p21.3). Most genes in the region are not labeled. **(A)** Each line represents a tumor, and deletions are noted in red (cases 1, 9, 11, 16, 18, and 20). **(B,C)** Probe plots of the deletions from cases 11 **(B)** and 16 **(C)**. Blue dots represent signals from individual probes, and black line segments represent averaged probe signals across a region

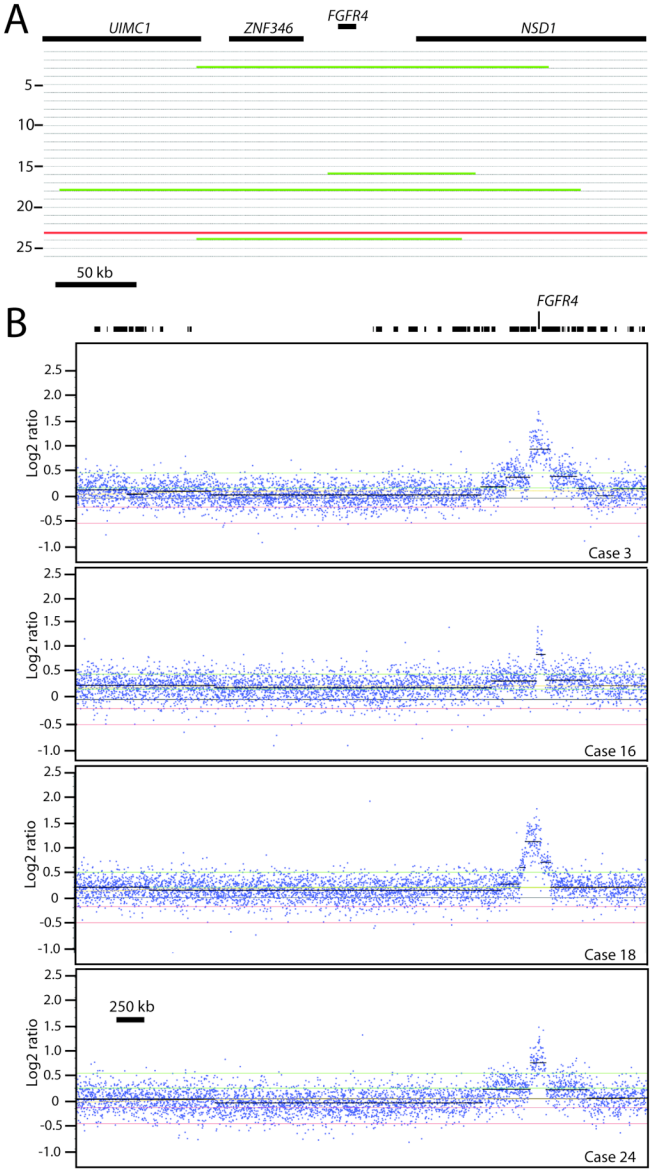

Figure 4: The *FGFR4* locus is amplified in ERMS.

Black bars above represent genes in the region (5q35.2-5q35.3). **(A)** Each horizontal line represents a tumor, with amplifications as green bars and a deletion as a red bar. **(B)** Probe plots of the four cases showing amplification of *FGFR4* (case 3, 16, 18, 24). *FGFR4* is the only gene in common in the amplified region, indicating that it is likely the target of the amplification. Blue dots represent signals from individual probes, and black line segments represent averaged probe signals across a region.

Table 5: *FGFR4* mutation and amplification status of ERMS

Tumor ID	Amino Acid Substitution	Amplification status
3	N535D	Amplified
14	V550L	
16	V550L	Amplified
18	V550L	Amplified
24	V550M	Amplified

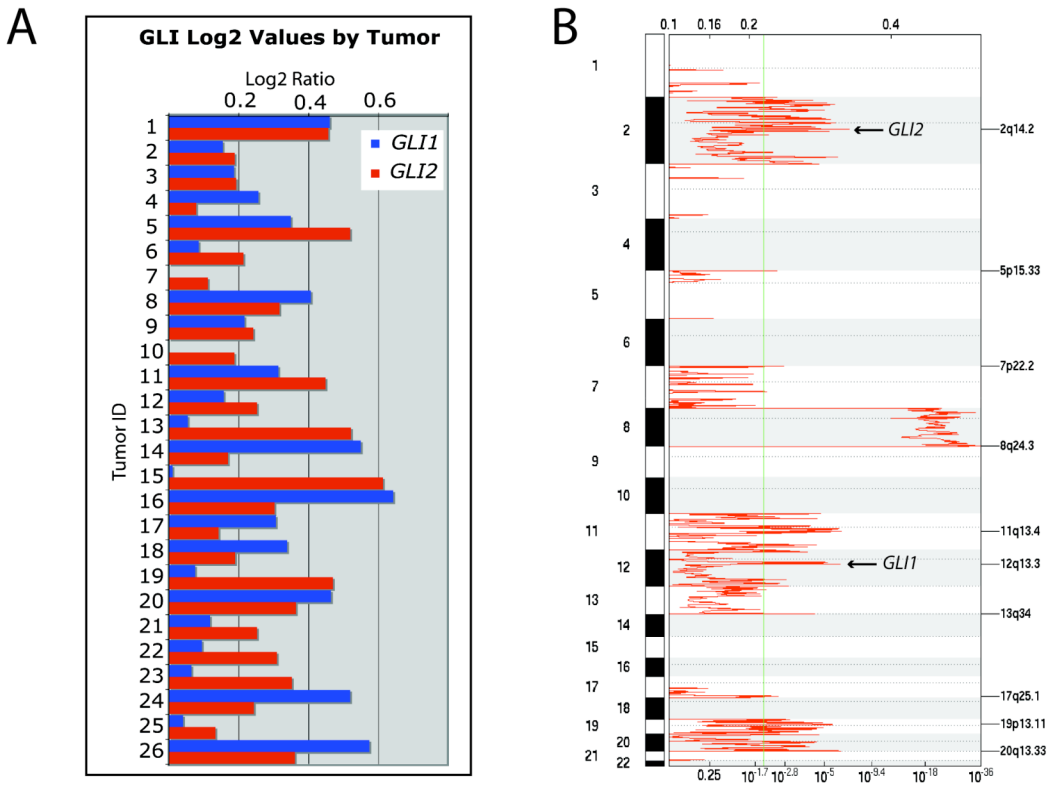

Figure 5: *GLI1* and *GLI2* are amplified in most ERMS tumors.

(A) Bar graph of log2 values from all 26 tumors for *GLI1* (blue) and *GLI2* (red). A normal copy number would have a log2 value of 0. **(B)** GISTIC plot of the statistical significance of regions of amplification. The regions including 2q14.2 (*GLI2*) and 12q13.3 (*GLI1*) are highlighted.

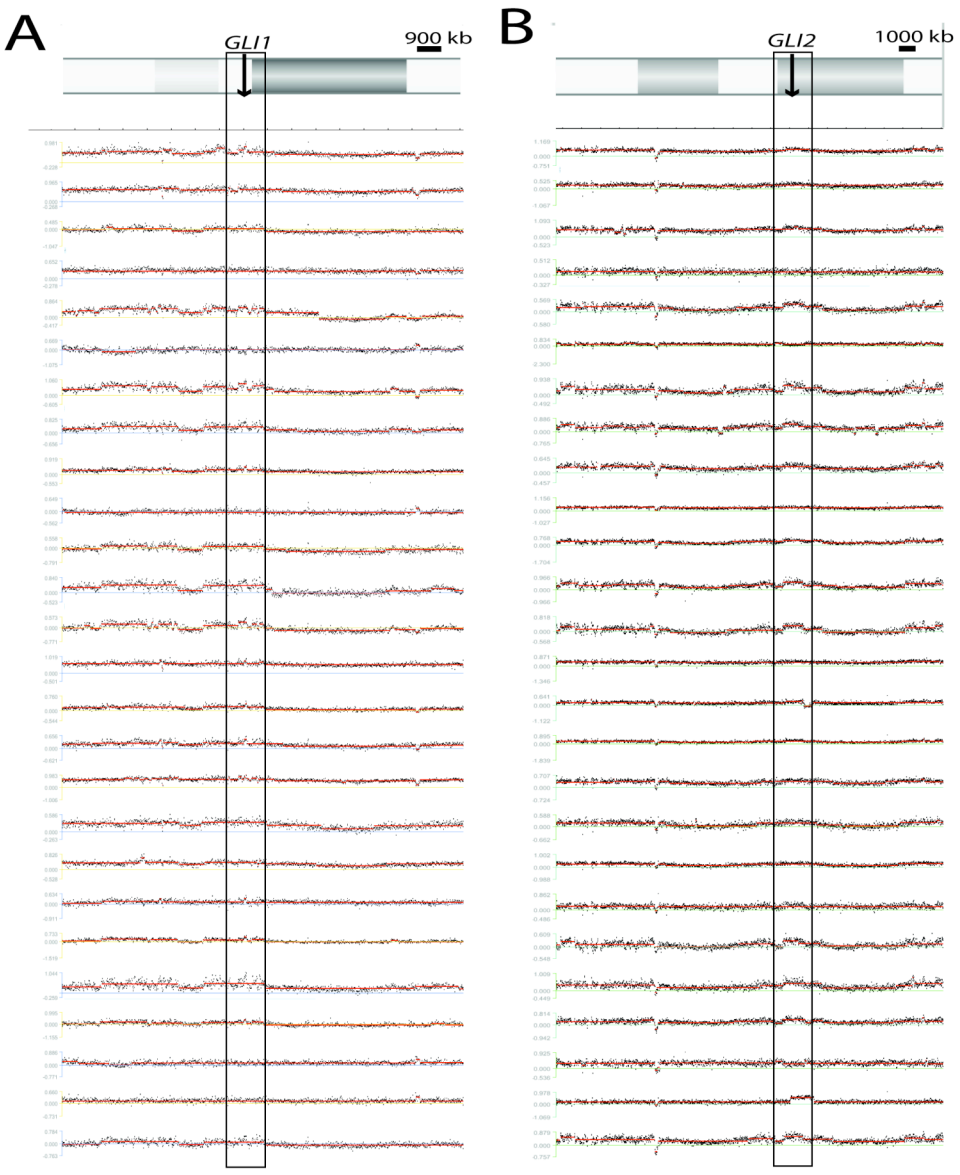

Figure 6: *GLI1* and *GLI2* are the likely targets in region 12q13.3 and 2q14.2, respectively.

Probe signals from region surrounding *GLI1* **(A)** and *GLI2* **(B)**, with each tumor as a single line. Baseline is at 0, Regions above the baseline are gains, and regions below the baseline are losses.

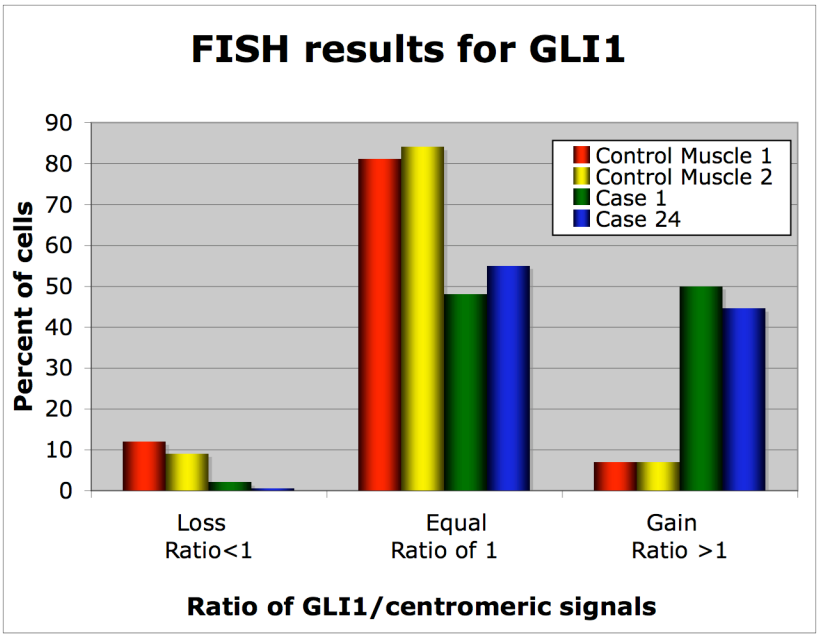

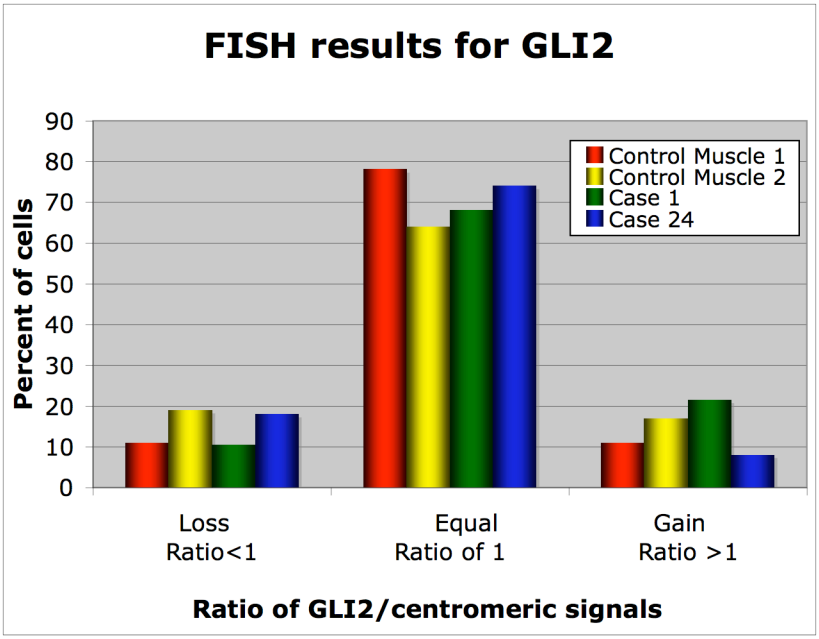

Figure 7: FISH confirmed gains of GLI1 (A) but not GLI2 (B).

Ratio of signals from region of interest GLI1 **(A)** and GLI2 **(B)** to their respective paracentromeric controls in FFPE embedded skeletal muscle and in indicated ERMS cases.

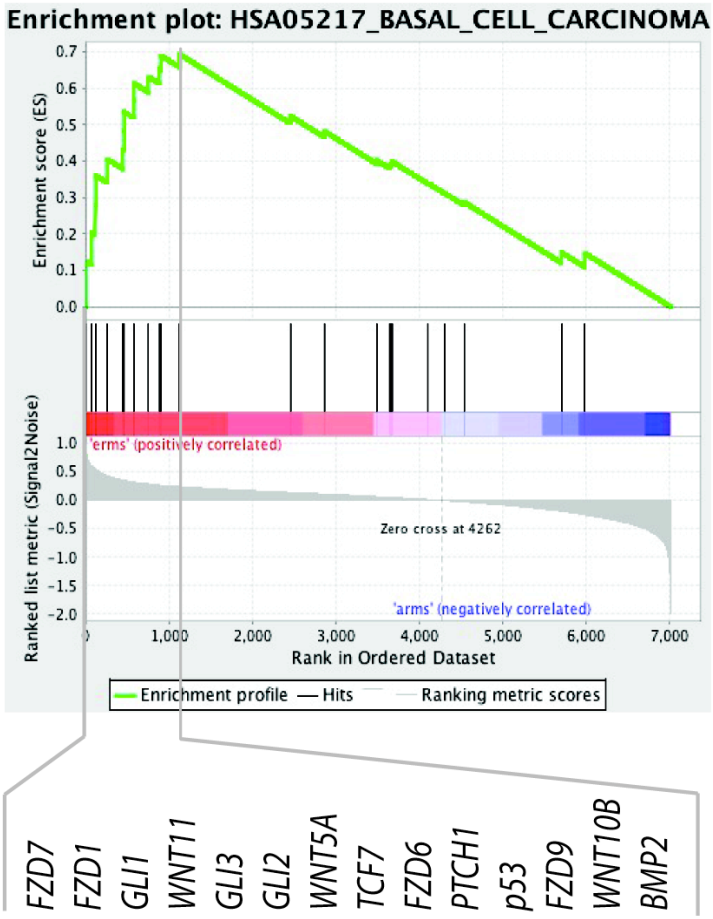

Figure 8: Hedgehog-associated Basal Cell Carcinoma signature is enriched in ERMS compared to ARMS

GSEA identifies enrichment of the basal cell carcinoma gene set (p-value<.001) when comparing gene expression patterns in ERMS with those from ARMS. Genes contributing to this enrichment are annotated beneath.

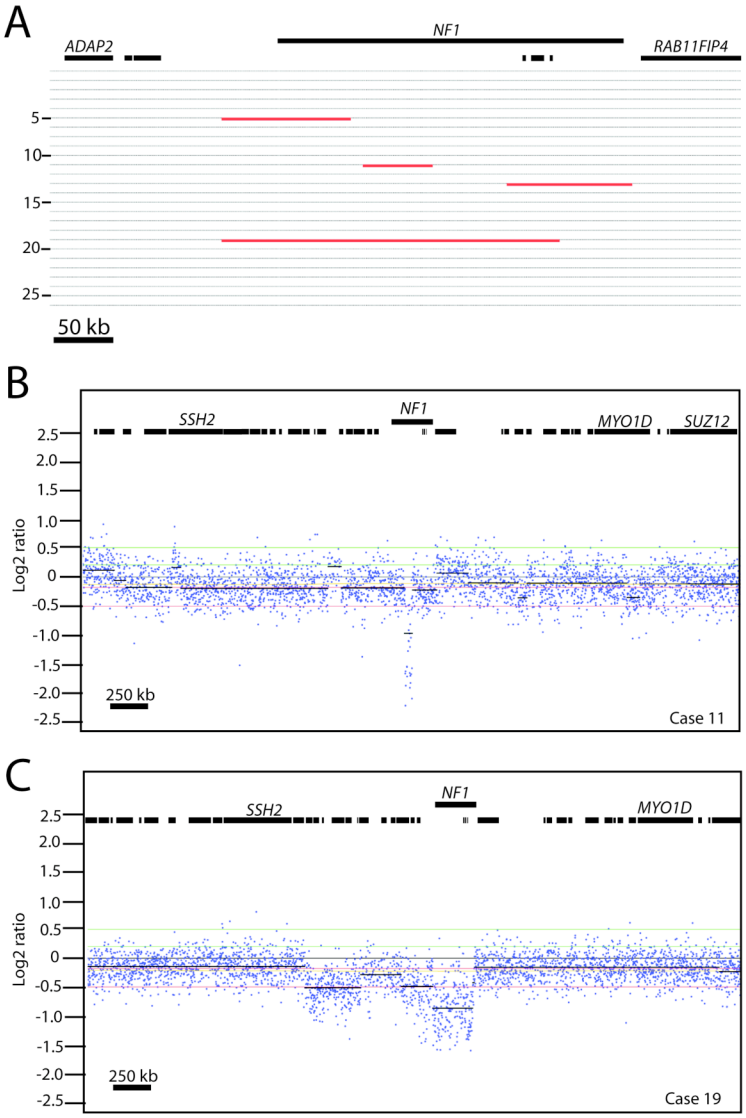

Figure 9: The *NF1* tumor suppressor is deleted in some ERMS.

Black bars above represent genes in the region (17q11.2). Most genes in the region are not labeled. There are additional small genes embedded within the large,~350 kb *NF1* locus (pictured under *NF1*). Some deletions also affect these genes, but aside from the *NF1* locus no single gene is affected by all four deletions, indicating that *NF1* is likely the target of the deletions. **(A)** Each line represents a tumor with focal deletions seen as red bars (cases 6, 11, 13, and 19). **(B)** Probe plot of case 11 and **(C)** case 19. Blue dots represent signals from individual probes, and black line segments represent averaged probe signals across a region.

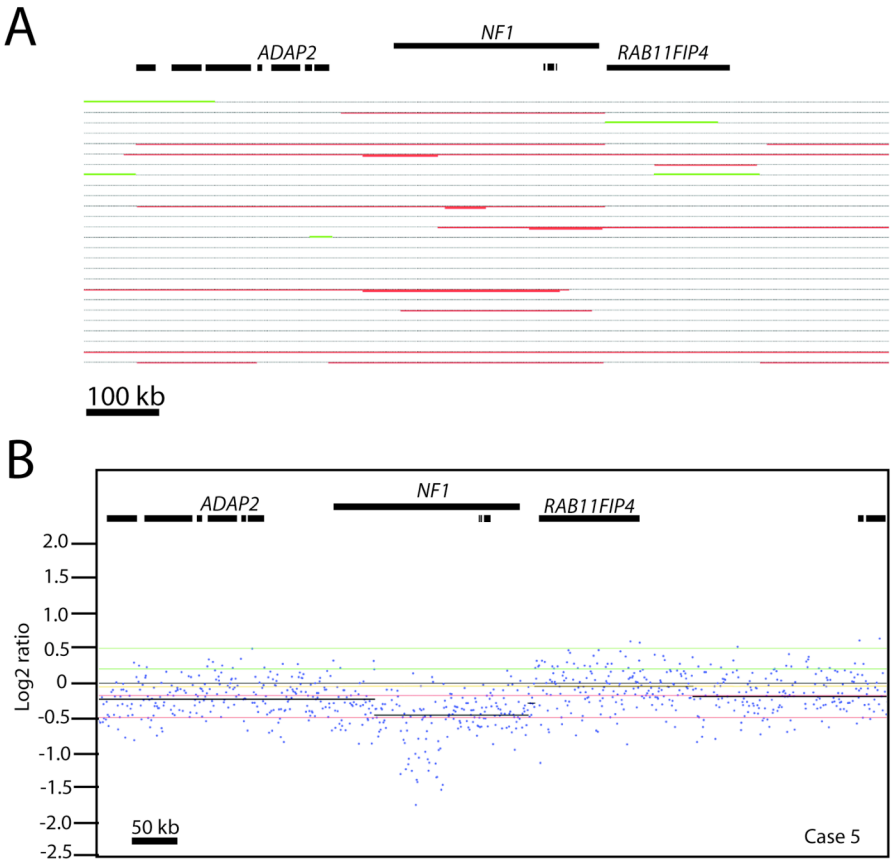

Figure 10: Additional ERMS patients show low-level deletion of *NF1*

Black bars above represent genes in the region (17q11.2). Not all genes in the region are labeled. There are additional genes embedded within the large, ~350 kb *NF1* locus (pictured under *NF1*). **(A)** Each line represents a tumor with deletions seen as red bars and gains seen as green bars. **(B)** Probe plot of case 5. Blue dots represent signals from individual probes, represent black line segments are averaged probe signals across a region.

Table 6: *NF1* deletion is an alternative method of *Ras* pathway activation in ERMS

Case ID	NF1 Status	Ras Mutation Status
2	Heterozygous deletion	Wild-type
5	Heterozygous deletion	Wild-type
21	Heterozygous deletion	Wild-type
6	Homozygous deletion	Wild-type
11	Homozygous deletion	Wild-type
13	Homozygous deletion	Wild-type
19	Homozygous deletion	Wild-type
1	Wild-type	NRAS G12C
4	Wild-type	NRAS Q61R
8	Wild-type	KRAS G12D
9	Wild-type	NRAS Q61H
10	Wild-type	NRAS Q61K
12	Wild-type	HRAS G13R
17	Wild-type	NRAS Q61K
20	Wild-type	HRAS G12C
22	Wild-type	NRAS Q61R
25	Heterozygous chromosomal loss	KRAS G12C
26	Heterozygous chromosomal loss	HRAS G13R NRAS G12D

Table 7: Summary of Patient Findings

Tumor ID	CDKN2A/B	FGFR4 Amp	FGFR4 Mut	NF1 Del	Ras Mut		GLI1	GLI2	Other	Status
1	X				NRAS	G12C	0.46	0.456		Alive
2							0.154	0.188		Alive
3		X	N535D				0.186	0.192		Alive
4					NRAS	Q61R	0.256	0.078		Alive
5							0.349	0.519		Alive
6				X			0.085	0.213		Dead
7							0	0.111		Alive
8					KRAS	G12D	0.406	0.316		Progression
9	X				NRAS	Q61H	0.216	0.241		Dead
10					NRAS	Q61K	0	0.187		Dead
11	X			X			0.313	0.448	PTEN	Alive
12					HRAS	G13R	0.157	0.252		Dead
13				X			0.054	0.521		Alive
14			V550L				0.549	0.169		Dead
15							0.01	0.613		Alive
16	X	X	V550L				0.642	0.302		Alive
17					NRAS	Q61K	0.306	0.142		Dead
18	X	X	V550L				0.338	0.189	BCL2L1	Dead
19				X			0.075	0.469		Progression
20	X				HRAS	G12C	0.464	0.363		Progression
21							0.117	0.252		Alive
22					NRAS	Q61R	0.094	0.309		Alive
23							0.064	0.352		Alive
24		X	V550M				0.519	0.243		Alive
25					KRAS	G12C	0.04	0.133		Alive
26					HRAS NRAS	G13R G12D	0.574	0.36		Dead

CHAPTER THREE: PILOT STUDY

INTRODUCTION:

As a proof of principle, prior to our characterization of the ERMS tumors, we isolated DNA from formalin-fixed paraffin embedded tumors and obtained aCGH data for two translocation-positive ARMS (*PAX3:FOXO1*) tumors and one ERMS tumor. We analyzed these tumors for copy number variation with and without the aid of the Nexus CGH software and identified regions of gain and loss as well as genes that may be critical for RMS pathogenesis or that might offer therapeutic targets. Several candidates for further study were proposed, but the most intriguing was POU3F3, a POU 3 homeodomain transcription factor with no known roles in oncogenesis or muscle development (McEvilly et al. 2002).

ALEVEOLAR RHABDOMYOSARCOMA

Alveolar RMS (ARMS) is typically seen in adolescents with disease of their extremities, and has a higher risk of metastasis or treatment-resistance. Disease pathogenesis is driven by a characteristic chromosomal translocation in 75% of cases; in these tumors the PAX3 or

PAX7 transcription factors are fused to the FOXO1 transcription factor (Xia et al. 2002). PAX3 and PAX7 proteins have critical roles in normal muscle development, and the fusion proteins use PAX DNA binding domains to drive aberrant muscle related malignancies via the transactivation domain of FOXO1 (Xia et al. 2002).

PAX3 AND PAX 7 IN MYOGENESIS

Myogenic regulatory factors (MRFs) are bHLH (basic helix-loop-helix) transcription factors that along with MEF2 and E proteins coordinate gene expression in normal muscle (De Giovanni et al. 2009). Muscle cell fate is specified by the MRFs, MYOD and MYF5, and differentiation by MRFs MYOD, MYF6, and MYOG. Terminal differentiation is characterized by the expression of MYOG and other contractile proteins (De Giovanni et al. 2009).

PAX3 is important in myogenic specification above and at the level of MYOD, and MYF5 expression (De Giovanni et al. 2009). PAX3 functions as an inhibitor of apoptosis, promotes myogenic proliferation and migration (Buckingham et al. 2003), and is necessary for muscle development, as mice that are PAX3 deficient fail to form hypaxial and epaxial muscle (Keller et al. 2004).

PAX7 deficient mice, by comparison, demonstrate normal embryonic muscle mass but an impaired ability to form muscle stem (satellite) cells (Keller et al. 2004). Satellite cells are progenitor cells that have escaped terminal differentiation and reside in the basal lamina; in the setting of injury, these cells are stimulated to proliferate, undergo terminal differentiation, and fuse to form muscle fibers (Hettmer and Wagers 2010).

PAX3/7:FOXO1 IN ARMS

PAX3/7:FOXO1 fusions are largely thought to be similar in the role of ARMS pathogenesis. Expression of the PAX3:FOXO1 fusion protein in myogenic precursors results in focus formation, anchorage independent growth, and transformation, findings not observed with PAX3 overexpression alone (Xia et al. 2009). These results suggest that the nuclear localized fusion protein has different transcription targets or differentially regulates the original PAX3 transcription targets, despite intact PAX3 DNA binding domains. Paradoxically, the PAX3:FOXO1 fusion protein is more potent than wild-type PAX3, though it is has poor DNA binding (Fredericks et al. 1995). This is due to the insensitivity of FOXO1 transactivation domain to the repressive function of the PAX3 N-terminus (Xia et al. 2009). Several studies reviewed in (De Giovanni et al. 2009) have used *in vitro* systems, RNAi in translocation-positive ARMS

and/or over-expression in cell lines, to propose candidate targets of the fusion protein and to determine the roles of the fusion protein in ARMS tumorigenesis. siRNA directed against the PAX3:FOXO1 fusion in tumor cells resulted in reduced motility, increased muscle differentiation, and decreased proliferation, due to the accumulation of cells in G1 (not via apoptosis as previously reported with use of siRNA directed against PAX3) (Kikuchi et al. 2008). *In vivo*, mouse models expressing PAX3:FOXO1 under control of the MYF6 promoter, a marker of terminal differentiation, develop ARMS (Keller et al. 2004).

Fred Barr recently showed that alveolar rhabdomyosarcoma requires high-level expression of the PAX3/7:FOXO1 fusion product for malignancy. *In vitro* cell cultures expressing low-levels of the PAX3:FOXO1 fusion protein were injected into mice and tumors arising from xenografts using these cultures uniformly displayed high-levels of the fusion protein (Xia et al. 2009). In ARMS tumors the PAX7:FOXO1 fusion is often genomically amplified and over-expressed. In contrast, PAX3:FOXO1 fusions are not typically amplified but are over-expressed, although the mechanism is unknown (Davis and Barr 1997).

METHODS

DNA ISOLATION FROM FFPE TUMORS

I isolated genomic DNA from formalin-fixed paraffin embedded tumors, 2 ARMS and 1 ERMS from Children's Medical Center of Dallas, using the DNEASY Kit (Qiagen) and a modified protocol described in (Maher et al. 2006). Samples were cut into 40 micron sections prior to being deparafinized in 3 washes of 1200 ul of xylene, followed by another 3 washes using 100% ETOH. After incubation at 37 degrees for 10 minutes, samples were then washed in 1200 ul PBS. The tissue pellet was suspended in buffer, and 40 ul of 10 mg/ml proteinase K (invitrogen) was added. Tumors were digested overnight at 55 degrees. Following the addition of 10 ul of 2 mg/ml RNASE and a 10 minute room-temperature incubation, 410 ul of AL buffer were added. Samples were incubated for 10 minutes at 70 degrees, and then following the addition of 410 ul of ETOH, columns were loaded with sample and centrifuged. Columns were washed with 500 ul of AW1 buffer and 500 ul of AW2 buffer, with centrifugation between each step at 8000 rpm for 1 min. Columns were eluted twice with 30 ul of AE buffer.

Genomic DNA concentration and quality was determined using a Nanodrop-1000 spectrophotometer (Nanodrop); all samples met strict cutoffs of 260/280 ≥ 1.8 and a 260/230 ≥ 1.9. Electrophoresis of 250 ng of genomic DNA on a 0.8 percent agarose gel confirmed a smear with greater than 50 percent of the material 10 kb or larger.

ROCHE NIMBLEGEN ARRAY COMPARATIVE GENOMIC HYBRIDIZATION (ACGH)

I sent 5 - 15 micrograms of genomic DNA to Roche NimbleGen (Reykjavik, Iceland) for aCGH using the 2.1 million probe platform (2.1 M), which utilizes genome-wide probe spacing of approximately every 1,110 bp, yielding an effective resolution of five to ten kilobases. We used pooled male reference genomic DNA provided by NimbleGen as comparitor DNA.

BIOINFORMATICS ANALYSIS

I imported normalized log2 probe signal values into Nexus Copy Number software (BioDiscovery) and segmented using a five-probe call with three percent outlier removal and a significance threshold of 1E-12. I defined low-level gain and loss as log2 values of 0.2 and -0.2 respectively

and high-level amplification and deletion as ±0.5. To identify regions of high-copy gain and loss, analysis of these tumors was also completed visually using Nimblescan (Roche).

GENOMIC Q-PCR

The McDermott center used 300 ng of normal skeletal muscle DNA and tumor DNA to measure RNASE-P and POU3F3 copy number using FAM-labeled Taqman probes (Applied Biosystems), this analysis was done in triplicate.

RNA ISOLATION FROM FFPE SAMPLES & CELL LINES

FFPE Samples: I isolated RNA from FFPE skeletal muscle and one ARMS tumor using the RecoverAll Kit (Ambion) with suggested modifications to the manufacturer's protocol, briefly, a 3-hour digest and a second DNase treatment prior to reverse transcriptase PCR and additional studies. Samples were again cut into 40 micron scrolls and 1 ml of xylene was added. After incubation at 50 degrees for 3 minutes, samples were centrifuged at maximum speed for 1 minute and the xylene decanted. Pellets were washed twice with EtOH before being allowed to aid-dry for 45 minutes. 100 ul of digestion buffer and 4 ul of proteinase K

were added, and the samples were incubated at 50 degrees for 3 hours and then 80 degrees for 15 minutes. 240 ul of isolation additive and 550 ul of ETOH were added, and the samples were passed through the column filter. Filters were washed with 700 ul of Wash 1 followed by 500 ul of Wash 2. DNase treatment was completed on the column (6 ul of Dnase buffer, 4 ul dnase, 50 ul H2O) at 30 minutes room temperature. Columns were again washed with 700 ul of Wash 1 and twice with 500 ul of Wash 2. RNA was eluted in 60 ul of Elution Buffer.

Cell Lines: I isolated RNA from cell lines using Trizol Reagent (Invitrogen) per manufacturer's protocol for cells in suspension, with the modification of a 30 minute room temperature incubation to precipitate RNA. Quality and quantity of RNA was measured using a Nanodrop-1000 spectrophotometer (Nanodrop), and 18S and 28S bands were observed on a 2% agarose gel.

REVERSE TRANSCRIPTION WITH SEMI-QUANTITATIVE/ REAL-TIME PCR

RNA was treated with DNase I (Invitrogen) and converted to cDNA using the High Capacity cDNA Reverse Transcription Kit (Applied Biosystems, Foster City, CA).

Semi-quantitative PCR of RNA from FFPE tumors: Template equal to 250 ng of RNA was used for semi-quantitative PCR using standard Taq protocol (NEB). POU3F3 forward and reverse primers were 5-TGGGCACACTCTACGGCAAC-3 and 5-TTGGGGCACTTGAGGAAG-3, respectively (anneal 58). Desmin primers were the kind gift of the Galindo Lab, UT Southwestern, forward primer 5-ACAACATTGCGCGCCTGGA-3 and reverse primer 5-AGCTTCCGGTAGGTGGCA-3 (anneal 65).

Semi-quantitative PCR of RNA from cell lines: Template equal to 250 ng of RNA was used for semi-quantitative PCR using standard Taq protocol (NEB). MYOD forward and reverse primers were 5-GCACCTGATAAATCGCATTG-3 and 5-CTGGGAAGGCAACAGACATA-3, respectively, (anneal 58) and the PAX3:FOXO1 fusion forward and

reverse primers were 5-CACCCCACATCTATTCCACAAGC-3 and 5-CCACTAATAGTACTAGCATTTGAG-3, respectively (anneal 60).

Real time PCR: An amount of cDNA corresponding to 50 ng of input RNA was used for each quantitative PCR reaction. Quantitative PCR was performed using the delta Ct method with Taqman probes on a 7900HT Fast Real-Time PCR System (Applied Biosystems) according to the manufacturer's instructions, using probes against GAPDH, PAX3, and PAX7 (Applied Biosystems).

PLASMIDS

pBabe & pBabe-eGFP: were a gift from Mark Hatley, M.D., Ph.D. of UT Southwestern Medical Center.

pBabe-PAX3:FOXO1: pCDNA3.1-PAX3:FOXO1, a gift from the Galindo Lab, UT Southwestern, was digested with SacI and FspI and the insert was blunted with Klenow and ligated into an EcoR1 digested, blunted pBabe vector. Colonies were screened using several test digests and validated with sequencing. Acknowledgements and thanks to Joo Hwang and Matthew Campbell, of UT Southwestern, for their assistance.

pBabe-POU3F3: POU3F3 as a 1.5 kb fragment bound by EcoR1 sites in pCMV5 was the kind gift of Diane Robbins, Department of Human Genetics University of Michigan medical school; it is described in (Malik et al. 1997). pBabe and POU3F3-pCMV5 were digested with EcoR1, ligated, screened, and sequenced, which revealed the absence of a start codon. Acknowledgements to Joo Hwang and Matthew Campbell, of UT Southwestern, for their assistance.

pBabe-FLAG:POU3F3: pBabe-POU3F3 was partially EcoR1 digested as were limiting dilutions of a duplex containing a start codon and coding flag sequence: 5-GGTGGTGAATTCACCATGGACTACAAAGA CGATGACGTAAGAATTCGGTGGT-3 and 5-ACCACCGAATTCTTTATC GTCATCGTCTTTGTAGTCCATGGTGAATTCACCACC-3'. Screening and sequencing verified a single insertion. Acknowledgements and thanks to Yi-Chun You, of UT Southwestern, for the design and construction of this plasmid.

pBabe-FLAGPOU3F3 DNA binding domain mutants: Mutagenesis of POU3F3 to abolish DNA binding was completed. From the vector pBabe:FLAGPOU3F3, a 1.2 kb XhoI/ClaI fragment containing Mus musculus POU3F3's DNA binding domain was cloned into pBlueScript II

SK (+) (Stratagene). Mutagenesis was performed using the Phusion Site-Directed Mutagenesis Kit (Finnzymes). To generate the mutation L418F, the following primers were used: 5-AACGCGCCTTTGACGCTAAC-3 and 5-CGAGAGCCACTTCCTCAAGTGCC-3. To generate the mutation R454P, the following primers were used: 5-GGTTGCAGAACCAG ACCCG-3 and 5-CACGCCAAAAGGAAAAACGC-3. Primers were 5' phosphorylated. PCR reactions were performed using 10 µL 5xPhusion Buffer, 5 µL dNTPs (2mM), 0.25 µL of each primer (100µM), 1 ng DNA template, 0.5 µL Phusion Polymerase, and H2O to 50 µL. Reactions were subjected to 98ºC for 30 seconds; 25 cycles of 98ºC for 10 seconds, 70ºC for 30 seconds, 72ºC for 1.5 minutes; 72ºC for 5 minutes. All portions of the 1.2 kb insert in pBluescript were sequenced to confirm the intended mutations were present and that there were no random mutations introduced. The 1.2 kb XhoI/ClaI fragments were then cloned into the original pBabe:FLAG:POU3F3 vector. The final construct was digested and partially sequenced to confirm accuracy. Acknowledgements and thanks to Jennifer Winn and Anqelica Sanchez, of UT Southwestern, for the generation of these plasmids.

CELL CULTURE

C2C12s and 293Ts were cultured in 17% FBS, 1% Pen/strep Highclone DMEM with glutamine and incubated under 5% CO2 at 37 degrees. To prevent confluence, cells were rinsed with PBS and trypsinized every 24-48 hours, and then plated at low density.

GENERATION OF VIRUS AND STABLE LINES

293Ts were plated onto a 10 cm dish to achieve 70-80% confluence the following day. A mixture of 6 ug of vector, 6 ug of pCL packing vector, and 36 ul of Fugene 6 (Roche-applied science) was brought up to a volume of 600 uL with serum free DMEM. This mixture was allowed to incubate 15 minutes at room temperature before being added drop wise to the plated 293Ts. After 24 hours, media was replaced, and at 48 and 72 hours, virus was harvested and polybrene was added to a final concentration of 8ug/ml. C2C12s at a confluency of 20-30% were infected with 3.5mls of viral media. Cells were selected using 15 ug/ml blasticidin for 2 days and then 5 days of 10 ug/ml.

WESTERN BLOTTING

Cells were harvested, lysed in RIPA buffer (150 mM NaCl, 1% IPEGAL (Sigma), 0.5% deoxycholate (Sigma), 0.1% SDS (Invitrogen), 50 mM Tris pH 8.0 (Sigma) with Complete protease inhibitor cocktail (Roche), and protein extract was quantitated against a standard BSA curve. 15 ug of protein for each cell line was denatured, run on a 12% Acrylamide Bis-Tris gel (Invitrogen), and transferred to nitrocellulose (Whatman) for western analyses. The membrane was blocked in 5% blotto, probed with primary Mouse anti-FLAG-M2 antibody (1:1000, Sigma), and secondary goat anti-mouse HRP-conjugated antibody (1:3000, Biorad), developed with ECL (Amersham), and exposed.

RESULTS AND DISCUSSION

CYTOGENETIC FINDINGS IN FFPE SAMPLES ARE CONSISTENT WITH THE LITERATURE

A global impression of the copy number abnormalities in the ARMS tumor, with gains and losses of at least a single copy number, is summarized in Figure 11. This data confirmed some of the large-scale changes described in the published examples of low-resolution CGH analysis of RMS, such as additional copies of chromosome 12.

PRELIMINARY DATA IDENTIFIED DISCRETE LOCI AND INDIVIDUAL GENES THAT MAY BE INVOLVED IN RMS.

aCGH revealed amplification of *CDK6*, an important regulator of cell cycle progression (G1/S transition). It is controlled by regulatory subunits including D-type cyclins and members of the INK4 family of CDK inhibitors. *CDK6* also phosphorylates and regulates activity of tumor suppressor *RB* (Cheng et al. 2004). It is known to be mutated in a number of cancers, including: retinoblastoma, T-cell leukemia, lymphoma, breast cancer, squamous cell carcinoma, melanoma, and glioblastoma (Cheng et al. 2004).

BMI1, a regulator of $p16^{INK4A}$ and $p19^{INK4D}$ cell cycle inhibitors, was also found amplified (Valk-Lingbeek et al. 2004). It is necessary for efficient self-renewal divisions of adult hematopoietic stem cell divisions (as well as PNS & CNS stem cells) (Valk-Lingbeek et al. 2004). It is activated by the Hedgehog pathway through both *SMO* and GLI (Valk-Lingbeek et al. 2004). *BMI1* is also involved in a number of cancers, including: CNS, bladder, skin, prostate, breast, ovarian, colorectal, lung, and hematological (Balasubramanian et al. 2009; Glinsky 2008; Raaphorst 2003; Valk-Lingbeek et al. 2004).

In ERMS, we identified loss of a small region that includes ten genes, two of which are well-validated tumor suppressors including *RASSF1* and *TUSC2* (Subramanian et al. 2008). This small region is often deleted in tumors and is postulated to be a tumor suppressor gene cluster. RASSF1A, an isoform of the *RASSF1* gene generated by alternative promoter use and splicing, is one of the most commonly inactivated tumor suppressors in cancer (Donninger et al. 2007). *RASSF1* is involved in a number of major cancer-relevant processes including apoptosis, genome instability and cell cycle control. Loss or inactivation of RASSF1 by RNAi stabilizes Cyclin D1 (Shivakumar et al. 2002). Our discovery of chromosomal loss of *RASSF1* in RMS is novel. However, allelic inactivation by promoter hypermethylation was described here at UT Southwestern by Dr. Michael White and Dr. John Minna in 60% of pediatric RMS tumor samples.

Finally, an amplicon containing only *POU3F3*, a POU-homeodomain transcription factor, was identified in an ARMS sample (Figure 12A). It is the only gene in an amplicon that was 25 kb in size and had an amplitude of greater than 0.8 suggesting multiple genomic copies. It has no known roles in myogenesis or oncogenesis.

POU3F3, A CANDIDATE FOR FURTHER ANALYSIS

POU3F3 is an intriguing candidate in the pathogenesis of translocation-positive ARMS. As stated previously it has no known roles in muscle or tumor formation. *POU3F3* (*BRN1*) is a POU domain transcription factors that controls radial migration of cortical layers II-V together with *POU3F2* (*BRN2*) (McEvilly et al. 2002; Sugitani et al. 2002). POU transcription factors are capable of forming homomeric and heteromeric complexes, prior to DNA binding, to alter protein interactions. These POU interaction partners include transcriptional activators and co-regulators, basal factors, and replicative factors (Malik et al. 1997). Remarkably, in developing spinal cord neurons POU3F3 directly activates PAX3 transcription (Pruitt et al. 2004). Studies identified four DNA elements necessary for PAX3 expression in a 1.6 kb promoter, Site A and B which bind HOX:PBX, and Site I (-1359 to -1334) and II (-856 to -827), which are non-consensus sequences (TGCC(A/T)TAAT(A/T)A) capable of binding POU3F3 and POU3F2 as monomers or dimers (Pruitt et al. 2004). In mice, the mutation of either binding site results in reduced expression of PAX3 throughout the neural tube (Pruitt et al. 2004). Our next step was to determine if this candidate was indeed amplified, and whether or not it was transcribed (as described next).

POU3F3 IS AMPLIFIED AND ACTIVELY TRANSCRIBED IN A SINGLE CASE OF ARMS

Quantitative genomic PCR verified amplification of *POU3F3*, with at least 4-5 copies on average per cell compared to the control *RNASE-P* (Figure 12B). This approximation is likely underestimated as the tumor also had gains in the region containing *RNASE-P*. Reverse transcriptase PCR detected *POU3F3* transcript in the tumor specimen but not in normal skeletal muscle (Figure 12C). This data confirmed that not only was the gene amplified at the genomic level, but it was also being actively transcribed. This immediately suggests the hypothesis that amplification and transcription of *POU3F3* might promote malignancy by driving over-expression of PAX3:FOXO1.

POU3F3 OVEREXPRESSION INDUCES EXPRESSION OF PAX3 IN PRIMITIVE MYOGENIC PRECURSOR CELLS

Cell lines expressing empty-vector, eGFP, PAX3:FOXO1, and FLAG:POU3F3 (as well as DNA binding mutants) were engineered (Figure 13 and Figure 14). We found that over-expression of POU3F3 in C2C12 myoblasts increased PAX3 expression 15-30 fold compared to cells with vector (Figure 15), and in preliminary studies appeared to

profoundly alter cellular morphology and differentiation. Whether PAX3 expression mediates these effects of POU3F3 over-expression, and whether POU3F3 over-expression can transform C2C12 cells, are major remaining questions.

SUMMARY OF REAGENTS GENERATED

The following plasmids have been obtained/engineered, packaged as virus, and used to obtain stable cell lines expressing their constructs: pBabe, pBabe-eGFP, pBabe-PAX3:FOXO1, pBabe-FLAG:POU3f3, pBabe-FLAG:POU3F3(L418F) and pBabe-FLAG:POU3F3(R454P).

Plasmids were confirmed with sequencing, and cell lines were confirmed with reverse-transcriptase PCR, in the case of PAX3:FOXO1 for which there is no satisfactory antibody, and by western blot using an anti-FLAG antibody for all POU3F3 constructs (Figure 13 and 14).

In light of our hypothesis concerning the direct binding of a PAX3 target sites by POU3F3, primers were designed for CHIP: Site I primers are 5-CGATAAGCCCTTTTGACTTCAG-3 and 5-TCTCCTTTGACAGTT TTGATGTG-3 and Site II primers are 5-CCTAGCCAAGACGTTGCTTC-3

and 5-TCTGAGAAGCGGGGACTTTA-3. The upstream primers for 4 kb are: 5-TCTGGGAGTTGGAATTCTGC-3 and 5-AGGCCTTCCCAGAGA GTCAT-3, and 2 kb are: 5-CCGGTTTAACCCACACATTC-3 and 5-TGGGGTAGAGGTTGCTTGAC-3. The downstream primers for regions downstream of the PAX3 promoter for 2 kb are 5-TCAACTCAAGTGGCATCTCG-3 and 5-AACCCCAGTCTCCTGCTTTT-3, while those for 4 kb are: 5-TGGCTAAGCAGAGGGACATT-3 and 5-AATAGGCGGATAGTGCGTTG-3. These primers give a single product on PCR.

These reagents were provided to Rene Galindo, M.D./Ph.D, of UT Southwestern.

Figure 11: Summary of copy number abnormalities in a PAX3:FOXO1 translocation-positive ARMS.

Low-level gains (green) and losses (red) are represented by a single bar, and high-level gains are represented by two. aCGH data are normalized to male reference.

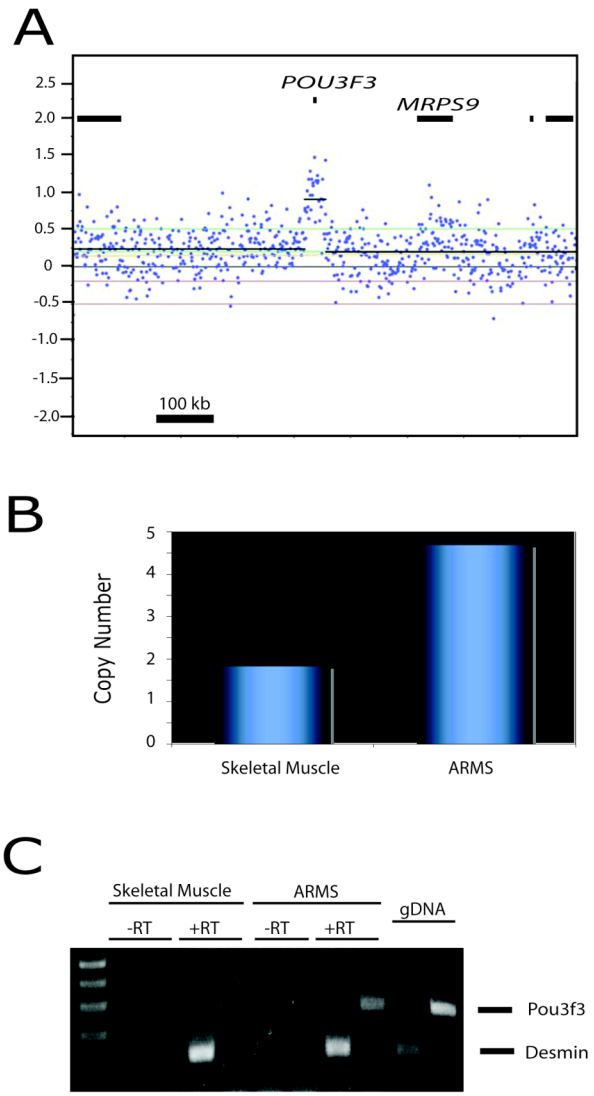

Figure 12: Amplification of a single gene, *POU3F3* in alveolar rhabdomyosarcoma was validated with qPCR, and its transcription was detected in tumor only.

(A) Blue dots represent probes across a small region of chromosome 2q12.1, and the black line is the segmentation of the probes. **(B)** qPCR confirmed at least 4-5 copies of *POU3F3* in the ARMS tumor compared to skeletal muscle. **(C)** Semi-quantitative reverse transcriptase PCR detected desmin (control) in skeletal muscle and ARMS, and detected POU3F3 transcription in ARMS only.

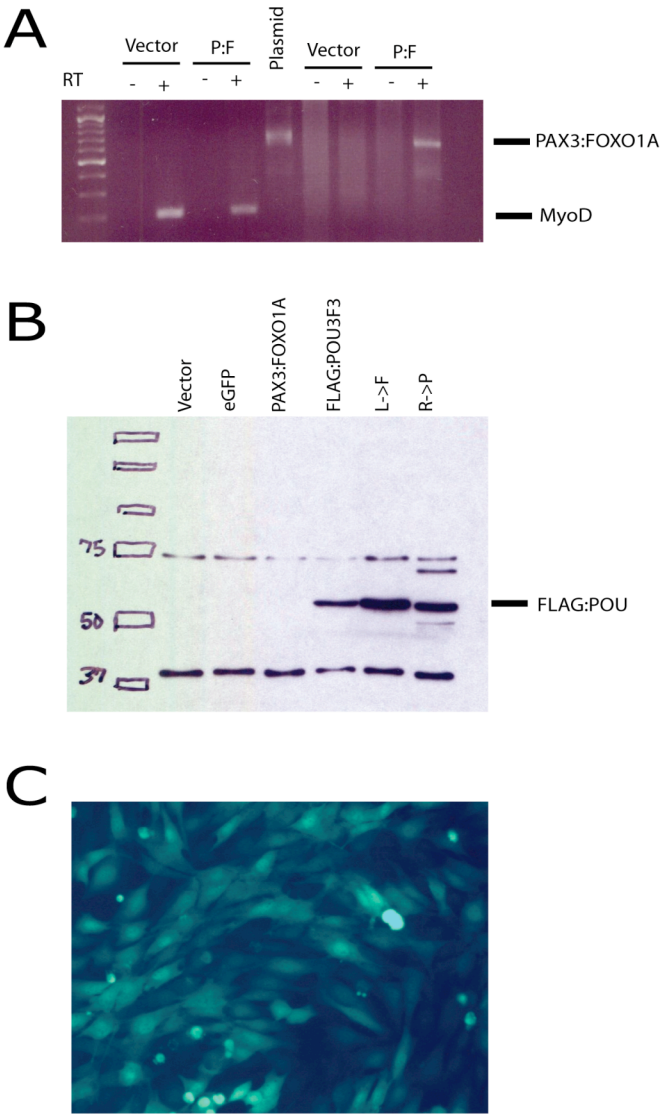

Figure 13: Stable cell lines express PAX3:FOXO1, FLAG:POU3F3, FLAG:POU3F3 DNA-binding mutants (L->F), (R->P), and eGFP.

(A) Semi-quantitative reverse transcriptase PCR detected MYOD (control) in vector and PAX3:FOXO1 expressing cells, and PAX3:FOXO1 in PAX3:FOXO1 expressing cells only. Plasmid template was used as a control. **(B)** Protein from cell lines was analyzed for expression of FLAG-tagged POU proteins. **(C)** GFP expression of eGFP cells.

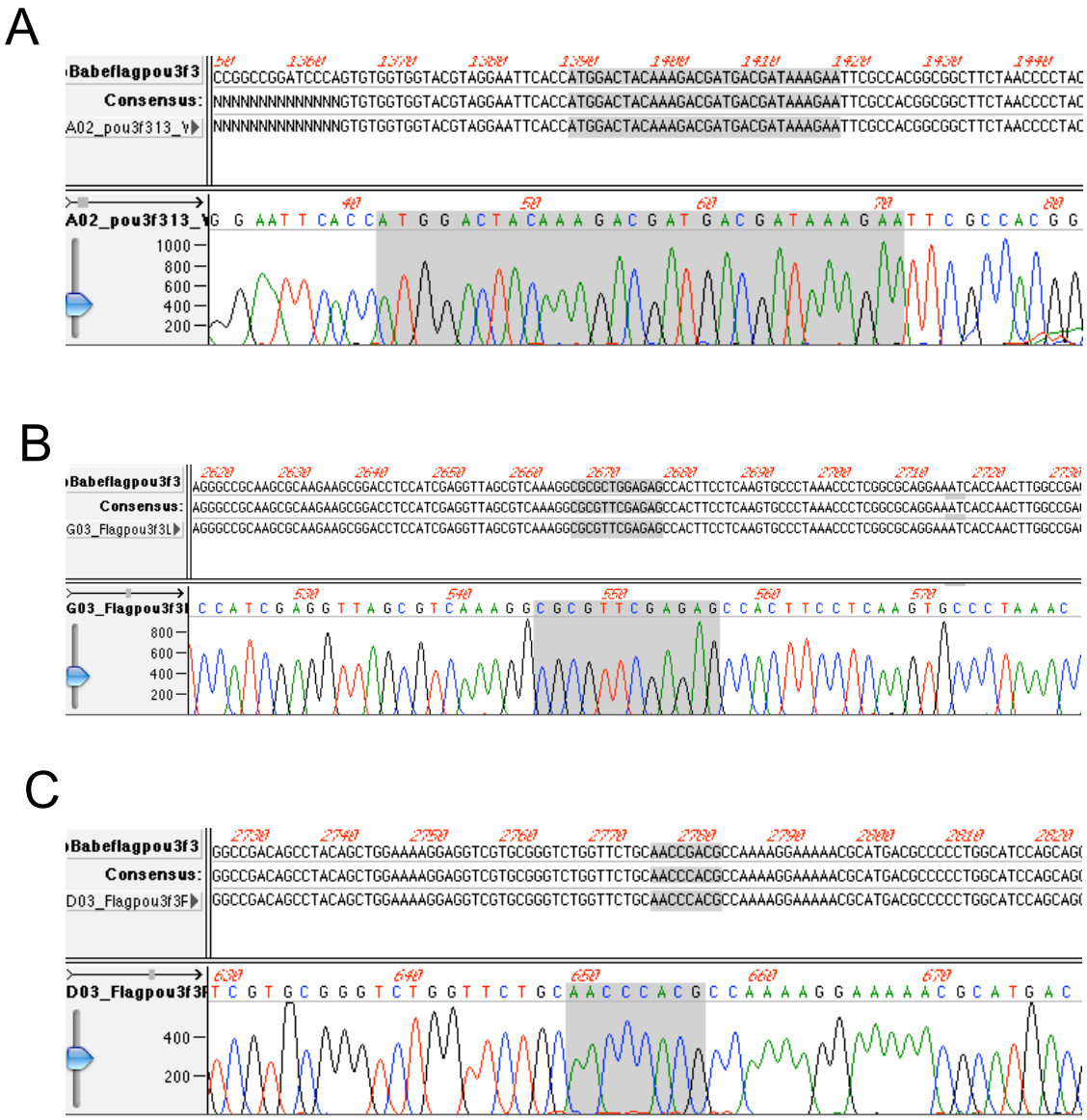

Figure 14: FLAG:POU3F3 DNA Binding mutants

Sequencing of FLAG:POU3f3 **(A)** Addition of start codon and FLAG-tag **(B &C)** Sequence of DNA binding mutants **(B)** FLAG:POU3F3: L418F mutant CTG->TTC mutation **(C)** FLAG:POU3F3: R454P mutant CGA->CCA mutation.

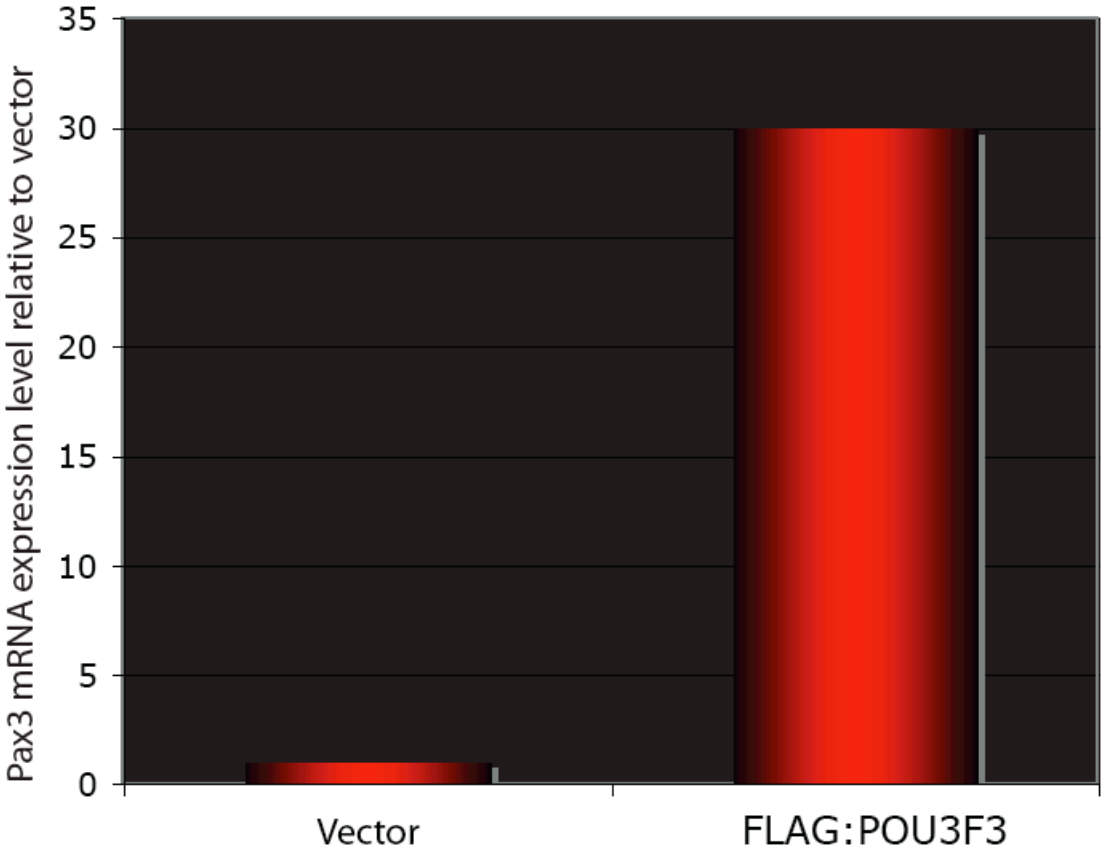

Figure 15: POU3F3 expression promotes PAX3 transcription and expression.

Real time qPCR of POU3F3 expressing cells demonstrate 30x overexpression of PAX3 compared to empty vector and eGFP.

CHAPTER FOUR: CONCLUSIONS

SUMMARY OF FINDINGS IN ERMS

Rhabdomyosarcoma is a muscle-related cancer that occurs primarily as two biologically distinct histological variants, embryonal (ERMS) and alveolar (ARMS). To learn what genomic changes drive ERMS pathogenesis, we used a new high-resolution array comparative genomic hybridization (aCGH) platform to examine the genomes of a specific subset of ERMS tumors, those from children with clinically-defined intermediate risk disease. Our data suggest that these tumors share a common genomic program that includes inactivation of the master regulator of the P53 and RB pathways, *CDKN2A/B*, and activation of *FGFR4*, Ras, and Hedgehog (Hh) signaling. We identified homozygous deletions of the *CDKN2A/B* tumor suppressor in 23% of patient samples and activation of *FGFR4*, a receptor tyrosine kinase, in 20% of patients, predominately by amplification of known, activating mutations. Over 90% of patients had low-level gains of the Hh-pathway transcription factors *GLI1* and/or *GLI2*, with a majority of tumors demonstrating gains of both genes, suggesting that Hh-pathway activation is characteristic of ERMS. Microdeletions affecting *NF1*, a tumor suppressor and inhibitor of Ras,

were also identified in 15% of tumor samples. Deletion of *NF1* and the presence of activating Ras mutations (in 42% of patients) were mutually exclusive, suggesting *NF1* loss is an alternative and potentially common mechanism of Ras activation in ERMS. Our data suggest that the tumors in children with intermediate-risk ERMS have similar genomic programs that drive development of their tumors. These findings have important implications for the application of targeted therapies to improve treatment of intermediate risk ERMS.

REMAING QUESTIONS IN THE IDENTIFICATION OF TARGETS UNDERLYING ERMS PATHOGENESIS

HOW COMMON IS RAS PATHWAY ACTIVATION?

The importance of Ras activation in RMS formation is supported by mouse models that utilize both *NF1* deletion (Vogel et al. 2000) and *KRAS* activation (Tsumura et al. 2006) to give rise to pleiomorphic RMS in the background of *P53* mutation. Ras pathway activation in spontaneous ERMS has previously been reported to occur in up to 50% of tumors, most commonly through activating mutations in *NRAS* and *KRAS* (Schaaf et al. 2010), with more rare mutations in *HRAS* and *PTPN11* (one case of 31) (Martinelli et al. 2009). No mutations, as of yet, have been reported in

RAF, *MEK1*, or *MEK*2 (Martinelli et al. 2009). Sequencing of our samples for mutations of *PTPN11, RAF*, and *MEK1/2*, might identify additional mechanisms of Ras pathway activation. Furthermore, in light of the findings in glioblastoma (Cancer Genome Atlas Research Network 2008), ovarian cancer (Sangha et al. 2008), and leukemia (Balgobind et al. 2008), it is reasonable to believe that tumors harboring heterozygous deletions of *NF1* may also have mutational inactivation of the remaining allele. It is also possible that additional tumors may have bi-allelic inactivation through mutation of both alleles. To determine how often NF1 is inactivated by these methods, sequencing of the coding regions is necessary. Alternatively, immunohistochemical studies of an RMS tissue microarray using antibodies directed against NF1 and its downstream signaling molecules pERK1/2 might also determine how often NF1 is inactivated in ERMS. To date, the commercially available antibodies designed for this purpose proved non-specific. Together, these studies could address how common Ras pathway activation is in cases of spontaneous ERMS.

HOW OFTEN ARE MEMBERS OF THE FGFR FAMILY MUTATED/AMPLIFIED OR ACTIVATED IN ERMS?

Members of the fibroblast growth factor family (FGFR) are commonly amplified, over-expressed, and mutated in a number of cancers, including prostate (Sahadevan et al. 2007), breast (Reis-Filho et al. 2006), gastric (Kunii et al. 2008), and bladder and cervical cancer (Cappellen et al. 1999), as well as glioblastoma (Rand et al. 2005), endometrial carcinoma (Pollock et al. 2007), and lung adenocarcinoma (Ding et al. 2008). In RMS, *FGFR1* amplification has been described in 11 percent (3/27) of translocation-negative ARMS and six percent (3/51) of ERMS (Williamson et al. 2010). Amplification of *FGFR4*, on the other hand, has not been previously been described in RMS, though activating mutations in three codons contained in the tyrosine kinase domain have (Taylor et al. 2009). These three codons, however, do not represent all possible FGFR activating mutations, as other mutations of FGFR have been described in a number of cancers. We might therefore suspect that sequencing of all coding exons of FGFR4, as well as FGFR1, FGFR2, FGFR3, might reveal additional samples with FGFR activation.

HOW COMMON IS HEDGEHOG PATHWAY ACTIVATION IN ERMS?

We have identified common low-copy number gains of *GLI1* and *GLI2* in a majority of ERMS tumors as well as a molecular signature consistent with Hedgehog pathway activation. As many tumors demonstrated gains in both *GLI1* and *GLI2*, it would be interesting to consider whether these tumors might also have mutations affecting other members of the Hedgehog pathway. In addition to amplification of regions containing *GLI1* (Bridge et al. 2002; Bridge et al. 2000; Goldstein et al. 2006), loss of heterozygosity and deletions in regions containing *PTCH1* and *SUFU* have been described in ERMS (Tostar et al. 2005). Other tumors associated with Hedgehog pathway activation have inactivating mutations in *PTCH1,* such as basal cell carcinoma (30-40%) and medulloblastoma (20%), and activating mutations of *SMO* in basal cell carcinoma (20%) and medulloblastoma (2%) (Lam et al. 1999). These mutations have not been described in spontaneously arising RMS tumors (Calzada-Wack et al. 2002). It would therefore be of interest to determine if our patient samples have mutations in these genes, in addition to their low-level gains of *GLI1* and *GLI2*.

GENOME SEQUENCING

We are currently arranging to send these samples for exome sequencing to identify additional mutations in these and other genes. We anticipate identification of genes involved in the pathways we have described above as well as the identification of many novel targets.

MOUSE MODELS FOR PRECLINICAL TESTING OF NOVEL THERAPEUTICS

Our findings suggest that there are common targetable mechanisms driving the pathogenesis of ERMS. The direction of therapies against these targets, to the patients most likely to benefit, will require the employment of a number of modalities in diagnosing pathway activation. The development of mouse models that are driven by the mutations identified in human tumors will be one approach to improve the preclinical testing of novel therapeutic approaches to rhabdomyosarcoma. Our data suggest that mouse models for ERMS should explore the incorporation of genetic lesions that activate the Ras, Hedgehog and *FGFR4* pathways, and that inactivate *CDKN2A/B*.

At present there are no mouse models of rhabdomyosarcoma that utilize combinations of the genetic lesions identified here, although many models make use of individual components including Ras activation, Hedgehog pathway activation, and inactivation of *CDKN2A*. RMS mouse models that utilize Ras activation, either by *KRAS* mutation or by heterozygous deletion of *NF1*, generate pleomorphic RMS in combination with *P53* inactivation (Langenau et al. 2007; Tsumura et al. 2006; Vogel et al. 1999). While mice with heterozygous inactivation of *NF1* and *P53* develop a myriad of tumors ranging from lymphoma to soft tissue sarcomas including RMS (eight percent of all tumors) (Vogel et al. 1999), mice with heterozygous inactivation of *P53* and targeted expression of mutant KRAS develop rhabdomyosarcomas in 100 percent of cases (Tsumura et al. 2006). These models, while supporting the function of Ras in generating RMS, do not recapitulate ERMS histology and suggest that Ras activation in combination with other lesions identified here may generate tumors that more closely resemble ERMS.

Mouse models of Hedgehog induced cancers, including mice heterozygous for loss of function mutations in *PTCH1 (Hahn et al. 1998),* heterozygous loss of *SUFU* in a P53-deficient background, (Lee et al. 2007), or that carry activating alleles of *SMO (Mao et al. 2006)*, also

develop ERMS at varying levels of penetrance. These models each validate the importance of Hedgehog pathway activation in development of ERMS, and in combination with genetic lesions identified here, may generate a mouse model that more closely resembles patient tumors.

RMS mouse models utilizing *CDKN2A* deletion and HGF/SF over-expression generate tumors that are histologically similar to ERMS in a majority of the mice (Sharp et al. 2002). We are unable to fully assess how often C-MET (HGF receptor) activation occurs in ERMS, but we have identified other pathways that are quite common, and suggest utilizing *CDKN2A/B* deletion with *FGFR4*, Ras, or Hedgehog activation in the development of additional or alternative ERMS models.

SUMMARY OF FINDINGS OF ARMS

Fred Barr recently showed that alveolar rhabdomyosarcoma requires high-level expression of the PAX3/7:FOXO1 fusion product for malignancy. For PAX7:FOXO1 fusions, this is often achieved by genomic amplification, but the mechanisms inducing the PAX3:FOXO1 fusion protein are unknown. In a pilot study using a single ARMS PAX3:FOXO1 translocation-positive tumor, we found an amplicon containing a single gene, *POU3F3*, a POU domain transcription factor. Quantitative genomic

PCR verified amplification of *POU3F3*, and reverse transcriptase PCR detected POU3F3 transcript in the tumor specimen but not in normal skeletal muscle. POU3F3 has no known oncogenic function or role in muscle development, but it is a direct activator of PAX3 transcription in developing spinal cord motor neurons. This suggested the hypothesis that *POU3F3* amplification might contribute to ARMS pathogenesis by driving high level expression of PAX3 and PAX3:FOXO1, a finding supported by our data showing increased PAX3 expression in stable muscle cell lines expressing POU3F3. Whether PAX3 expression mediates the effects of POU3F3 over-expression, and whether POU3F3 over-expression can transform C2C12 cells, are major remaining questions.

FUTURE DIRECTIONS IN ARMS

IS POU3F3 AMPLIFICATION CASE SPECIFIC OR TUMOR SPECIFIC?

In a single case of PAX3:FOXO1 translocation-positive ARMS, we identified amplification of POU3F3 and proposed that it might be responsible for expression of high-levels of the PAX3:FOXO1 fusion protein in our patient. It remains to be determined whether this finding is specific to this single case of ARMS or whether it is tumor specific. Unfortunately the expression data available (Davicioni et al. 2009) shows

relatively uniform expression of POU3F3 in translocation positive and negative ARMS, ERMS, and other soft tissue sarcomas. Whether this observation reflects the lack of POU3F3 over-expression in ARMS tumors remains a key question, one that more direct analysis of POU3F3 transcript levels or immunohistochemical studies might answer.

DOES POU3F3 DIRECTLY REGULATE PAX3 EXPRESSION IN VIVO TO PROMOTE TUMORIGENESIS?

As previously described, studies identified 4 DNA elements necessary for PAX3 expression in a 1.6 kb promoter, Site A and B which bind HOX:PBX, and Site I (-1359 to -1334) and II (-856 to -827), which are non-consensus sequences (TGCC(A/T)TAAT(A/T)A) capable of binding POU3F3 and POU3F2 as monomers or dimers (Pruitt et al. 2004). Preliminary analysis demonstrates that expression of POU3F3 in stable cell lines was associated with upregulation of PAX3, and was found to profoundly alter cell morphology and differentiation. Primers were designed to amplify these sites of interest, as well as sites two and four kb up-stream and down-stream of the PAX3 promoter for use in CHIP, to determine if POU3F3 directly up-regulates the observed increase in PAX3 expression in the myogenic precursors, C2C12. Additional studies are

needed to further evaluate the phenotype of myogenic precurors and to determine whether POU3F3 directly regulates PAX3 expression *in vivo*.

APPENDIX

Appendix A: FGFR4 mutants

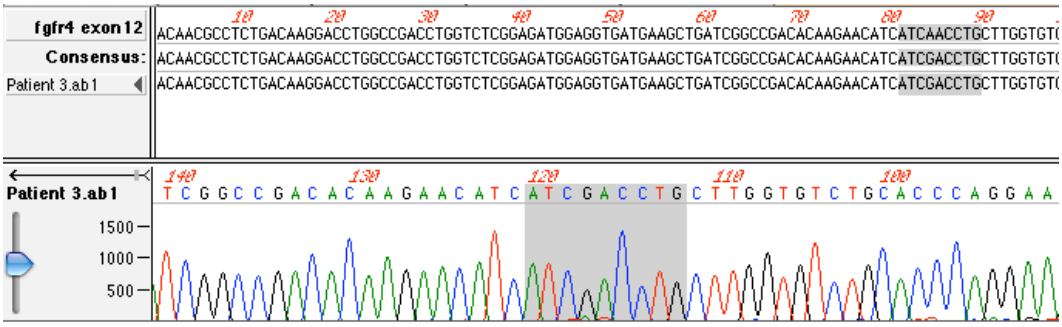

FGFR4 Exon 12: Patient 3

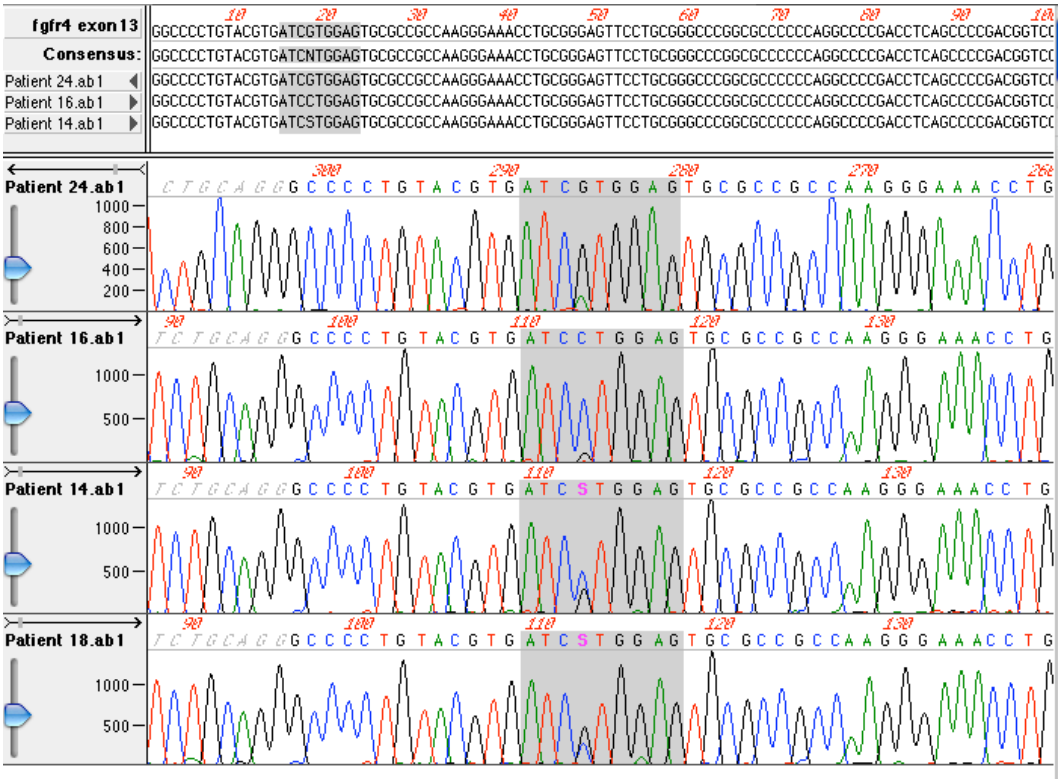

Mutations of FGFR4 Exon 13: Patient 14, 16, 18, and 24

Appendix B: Ras mutants

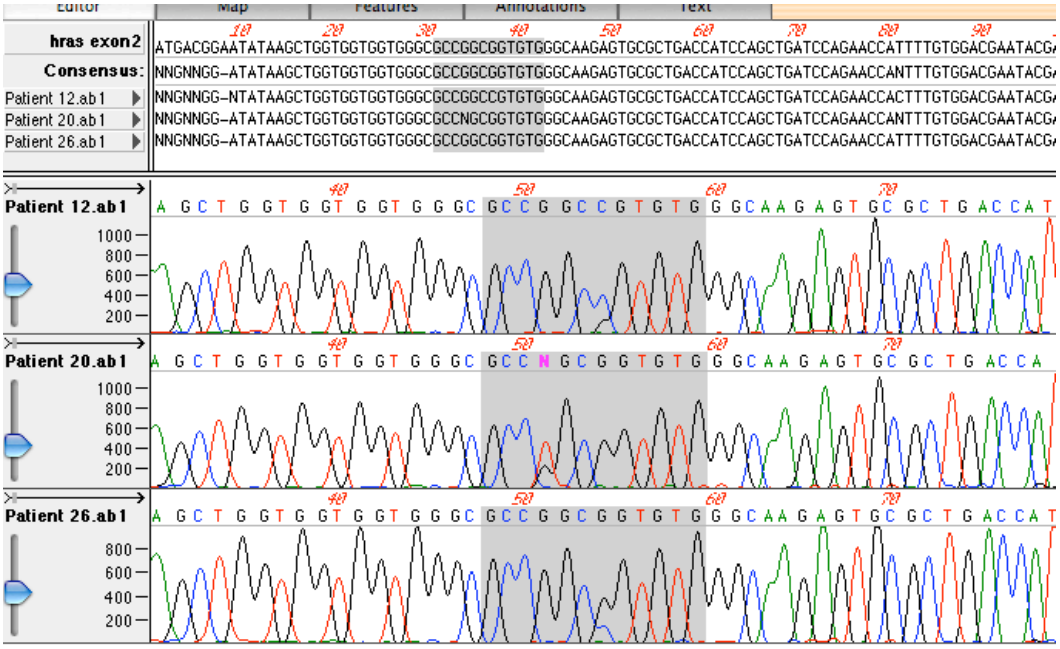

HRAS Exon 2: Patient 12, 20 and 26

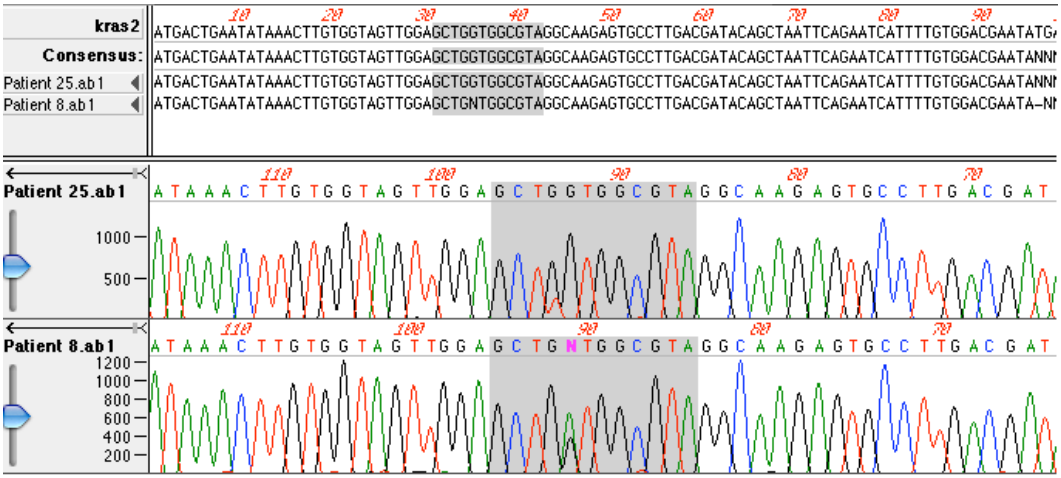

KRAS Exon 2: Patient 8 and 25

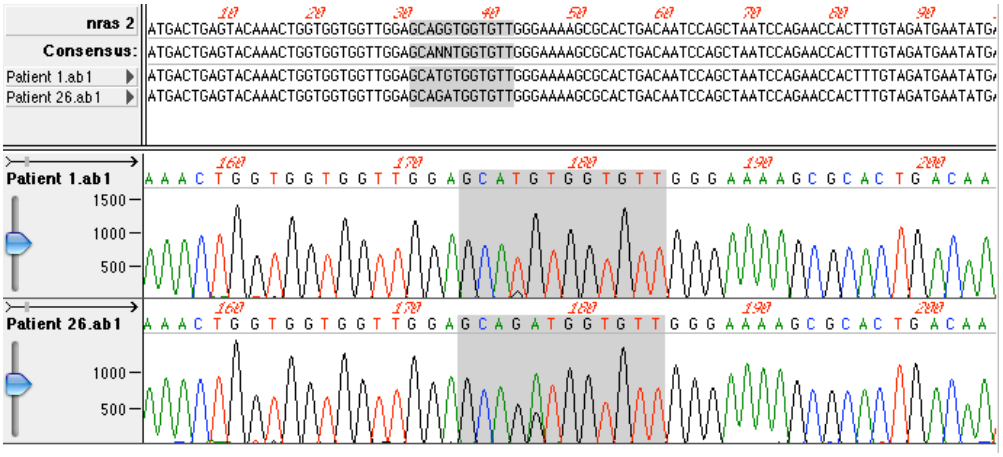

NRAS Exon 2: Patient 1 and 26

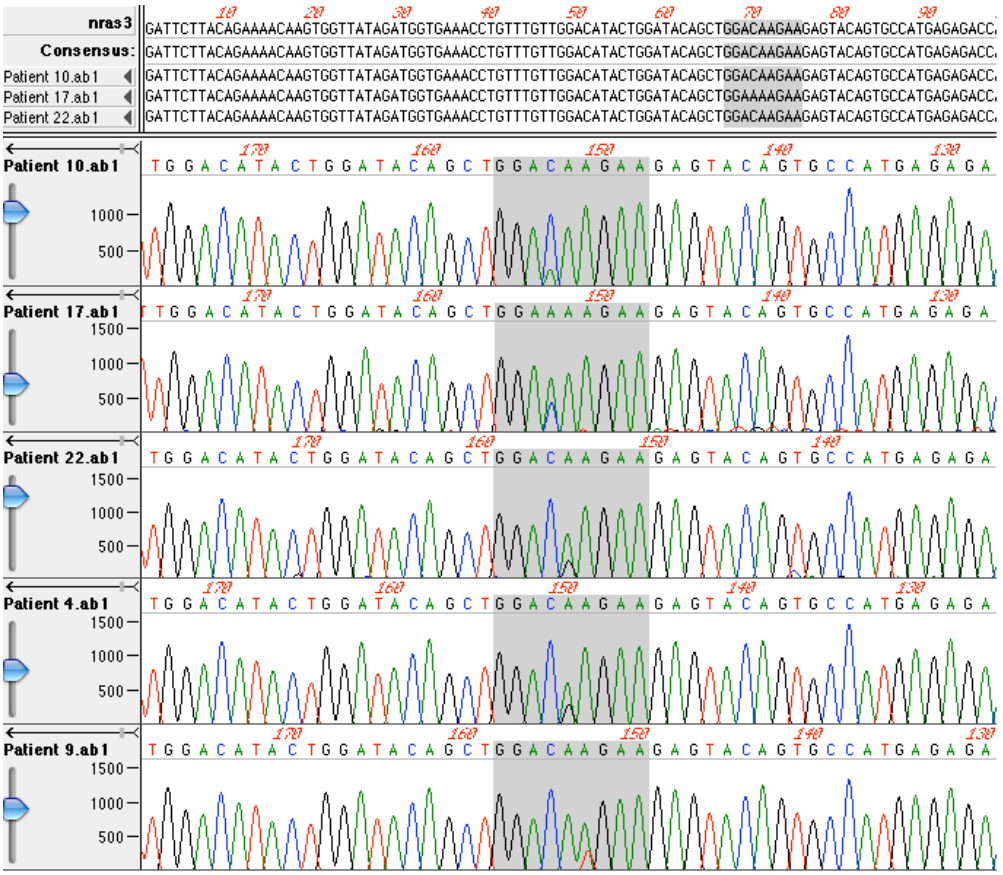

NRAS Exon 3: Patient 4, 9, 10, 17, and 22

LITERATURE CITED:

Arlt MF, Mulle JG, Schaibley VM, Ragland RL, Durkin SG, Warren ST, Glover TW. 2009. Replication Stress Induces Genome-wide Copy Number Changes in Human Cells that Resemble Polymorphic and Pathogenic Variants. The American Journal of Human Genetics 84(3):339-350.

Balasubramanian S, Adhikary G, Eckert RL. 2009. The Bmi-1 Polycomb Protein Antagonizes the (-)-Epigallocatechin-3-Gallate Dependent Suppression of Skin Cancer Cell Survival. Carcinogenesis.

Balgobind BV, Van Vlierberghe P, van den Ouweland AMW, Beverloo HB, Terlouw-Kromosoeto JNR, van Wering ER, Reinhardt D, Horstmann M, Kaspers GJL, Pieters R and others. 2008. Leukemia-associated NF1 inactivation in patients with pediatric T-ALL and AML lacking evidence for neurofibromatosis. Blood 111(8):4322-4328.

Beroukhim R, Getz G, Nghiemphu L, Barretina J, Hsueh T, Linhart D, Vivanco I, Lee JC, Huang JH, Alexander S and others. 2007. Assessing the significance of chromosomal aberrations in cancer: methodology and application to glioma. Proc Natl Acad Sci USA. p 20007-12.

Beroukhim R, Mermel CH, Porter D, Wei G, Raychaudhuri S, Donovan J, Barretina J, Boehm JS, Dobson J, Urashima M and others. 2010. The landscape of somatic copy-number alteration across human cancers. Nature. p 899-905.

Bouron-Dal Soglio De, Rougemont A-L, Absi R, Giroux L-M, Sanchez R, Barrette Sp, Fournet J-C. 2009. Beta-Catenin Mutation Does Not Seem to Have an Effect on the Tumorigenesis of Pediatric Rhabdomyosarcomas. Pediatric and Developmental Pathology 12(5):371-373.

Bridge, Liu, Qualman, Suijkerbuijk, Wenger, Zhang, Wan, Baker, Sorensen, Barr. 2002. Genomic gains and losses are similar in genetic and histologic subsets of rhabdomyosarcoma, whereas amplification predominates in embryonal with anaplasia and alveolar subtypes. Genes Chromosomes Cancer. p 310-21.

Bridge, Liu, Weibolt, Baker, Perry, Kruger, Qualman, Barr, Sorensen, Triche and others. 2000. Novel genomic imbalances in embryonal rhabdomyosarcoma revealed by comparative genomic hybridization and fluorescence in situ hybridization: an intergroup rhabdomyosarcoma study. Genes Chromosomes Cancer. p 337-44.

Buckingham M, Bajard L, Chang T, Daubas P, Hadchouel J, Meilhac S, Montarras D, Rocancourt D, Relaix F. 2003. The formation of skeletal muscle: from somite to limb. J Anat. p 59-68.

Calzada-Wack J, Schnitzbauer U, Walch A, Wurster KH, Kappler R, Nathrath M, Hahn. 2002. Analysis of the PTCH coding region in human rhabdomyosarcoma. Hum Mutat. p 233-4.

Cappellen D, De Oliveira C, Ricol D, de Medina S, Bourdin J, Sastre-Garau X, Chopin D, Thiery JP, Radvanyi F. 1999. Frequent activating mutations of FGFR3 in human bladder and cervix carcinomas. Nat Genet 23(1):18-20.

Chen Y, Takita J, Mizuguchi M, Tanaka K, Ida K, Koh K, Igarashi T, Hanada R, Tanaka Y, Park M-J and others. 2007. Mutation and expression analyses of the *MET* and *CDKN2A* genes in rhabdomyosarcoma with emphasis on *MET* overexpression. Genes, Chromosomes and Cancer 46(4):348-358.

Cheng KW, Lahad JP, Kuo WL, Lapuk A, Yamada K, Auersperg N, Liu J, Smith-McCune K, Lu KH, Fishman D and others. 2004. The RAB25 small GTPase determines aggressiveness of ovarian and breast cancers. Nat Med. p 1251-6.

Davicioni E, Anderson M, Finckenstein F, Lynch J, Qualman S, Shimada H, Schofield D, Buckley J, Meyer, Sorensen P and others. 2009. Molecular Classification of Rhabdomyosarcoma--Genotypic and Phenotypic Determinants of Diagnosis. A Report from the Children's Oncology Group. American Journal of Pathology. p 15.

Davis RJ, Barr. 1997. Fusion genes resulting from alternative chromosomal translocations are overexpressed by gene-specific mechanisms in alveolar rhabdomyosarcoma. Proc Natl Acad Sci USA. p 8047-51.

De Giovanni C, Landuzzi L, Nicoletti G, Lollini P, Nanni P. 2009. Molecular and cellular biology of rhabdomyosarcoma. Future Oncology. p 1449-1475.

Diller L, Sexsmith E, Gottlieb A, Li FP, Malkin D. 1995. Germline p53 mutations are frequently detected in young children with rhabdomyosarcoma. The Journal of Clinical Investigation 95(4):1606-1611.

Ding L, Getz G, Wheeler DA, Mardis ER, McLellan MD, Cibulskis K, Sougnez C, Greulich H, Muzny DM, Morgan MB and others. 2008. Somatic mutations affect key pathways in lung adenocarcinoma. Nature 455(7216):1069-1075.

Donninger H, Vos MD, Clark GJ. 2007. The RASSF1A tumor suppressor. J Cell Sci 120(18):3163-3172.

Dudka AA, Sweet SMM, Heath JK. 2010. Signal Transducers and Activators of Transcription-3 Binding to the Fibroblast Growth Factor Receptor Is Activated by Receptor Amplification. Cancer Res 70(8):3391-3401.

Felix, Kappel, Mitsudomi, Nau, Tsokos, Crouch, Nisen, Winick, Helman. 1992. Frequency and diversity of p53 mutations in childhood rhabdomyosarcoma. Cancer Res. p 2243-7.

Ferrari A, Bisogno G, Macaluso A, Casanova M, D'Angelo P, Pierani P, Zanetti I, Alaggio R, Cecchetto G, Carli. 2007. Soft-tissue sarcomas in children and adolescents with neurofibromatosis type 1. Cancer. p 1406-12.

Flaherty KTa, Hodi FSb, Bastian BCc. 2010. Mutation-driven drug development in melanoma. Current Opinion in Oncology May 2010;22(3):178-183(1040-8746).

Fredericks WJ, Galili N, Mukhopadhyay S, Rovera G, Bennicelli J, Barr FG, Rauscher FJ. 1995. The PAX3-FKHR fusion protein created by the t(2;13) translocation in alveolar rhabdomyosarcomas is a more potent transcriptional activator than PAX3. Mol Cell Biol. p 1522-35.

Gailani MR, Stahle-Backdahl M, Leffell DJ, Glyn M, Zaphiropoulos PG, Unden AB, Dean M, Brash DE, Bale AE, Toftgard R. 1996. The role of the human homologue of Drosophila patched in sporadic basal cell carcinomas. Nat Genet 14(1):78-81.

Gazdar AF, Minna JD. 2008. Deregulated EGFR Signaling during Lung Cancer Progression: Mutations, Amplicons, and Autocrine Loops. Cancer Prevention Research 1(3):156-160.

Gerber, Wilson, Li, Chuang. 2007. The hedgehog regulated oncogenes Gli1 and Gli2 block myoblast differentiation by inhibiting MyoD-mediated transcriptional activation. Oncogene. p 1122-36.

Glinsky GV. 2008. "Stemness" genomics law governs clinical behavior of human cancer: implications for decision making in disease management. J Clin Oncol. p 2846-53.

Goldstein, Meller, Issakov, Orr-Urtreger. 2006. Novel Genes Implicated in Embryonal, Alveolar, and Pleomorphic Rhabdomyosarcoma: A Cytogenetic and Molecular Analysis of Primary Tumors. NEO. p 332-343.

Gordon, McManus, Anderson, Min, Swansbury, Pritchard-Jones, Shipley, Group UkCCS, Group UKCC. 2001. Cytogenetic abnormalities in 42 rhabdomyosarcoma: a United Kingdom Cancer Cytogenetics Group Study. Med Pediatr Oncol. p 259-67.

Hahn, Wojnowski, Specht, Kappler, Calzada-Wack, Potter, Zimmer, Müller, Samson, Quintanilla-Martinez. 2000. Patched target Igf2 is indispensable for the formation of medulloblastoma and rhabdomyosarcoma. J Biol Chem. p 28341-4.

Hahn, Wojnowski, Zimmer, Hall, Miller, Zimmer. 1998. Rhabdomyosarcomas and radiation hypersensitivity in a mouse model of Gorlin syndrome. Nat Med. p 619-22.

Hart KC, Robertson SC, Kanemitsu MY, Meyer AN, Tynan JA, Donoghue DJ. 2000. Transformation and Stat activation by derivatives of FGFR1, FGFR3, and FGFR4. Oncogene. p 3309-20.

Hayes-Jordan A, Andrassy R. 2009. Rhabdomyosarcoma in children. Curr Opin Pediatr. p 373-8.

Hettmer S, Wagers AJ. 2010. Muscling in: Uncovering the origins of rhabdomyosarcoma. Nat Med 16(2):171-173.

Hoseong Yang S, Andl T, Grachtchouk V, Wang A, Liu J, Syu L-J, Ferris J, Wang TS, Glick AB, Millar SE and others. 2008. Pathological responses to oncogenic Hedgehog signaling in skin are dependent on canonical Wnt/[beta]-catenin signaling. Nat Genet 40(9):1130-1135.

Imai K, Takaoka A. 2006. Comparing antibody and small-molecule therapies for cancer. Nat Rev Cancer 6(9):714-727.

Iolascon, Faienza, Coppola, Rosolen, Basso, Ragione D, Schettini. 1996. Analysis of cyclin-dependent kinase inhibitor genes (CDKN2A, CDKN2B, and CDKN2C) in childhood rhabdomyosarcoma. Genes Chromosomes Cancer. p 217-22.

Jiang, Hui. 2008. Hedgehog Signaling in Development and Cancer. Dev Cell. p 801-812.

Johnson RL, Rothman AL, Xie J, Goodrich LV, Bare JW, Bonifas JM, Quinn AG, Myers RM, Cox DR, Epstein EH, Jr. and others. 1996. Human Homolog of patched, a Candidate Gene for the Basal Cell Nevus Syndrome. Science 272(5268):1668-1671.

Kanehisa M, Araki M, Goto S, Hattori M, Hirakawa M, Itoh M, Katayama T, Kawashima S, Okuda S, Tokimatsu T and others. 2008. KEGG for linking genomes to life and the environment. Nucl. Acids Res. 36(suppl_1):D480-484.

Keller, Hansen, Coffin, Capecchi. 2004. Pax3:Fkhr interferes with embryonic Pax3 and Pax7 function: implications for alveolar rhabdomyosarcoma cell of origin. Genes & Development. p 2608-13.

Khan J, Wei JS, Ringnér M, Saal LH, Ladanyi, Westermann F, Berthold F, Schwab M, Antonescu CR, Peterson C and others. 2001. Classification and diagnostic prediction of cancers using gene expression profiling and artificial neural networks. Nat Med. p 673-9.

Kikuchi K, Tsuchiya K, Otabe O, Gotoh T, Tamura S, Katsumi Y, Yagyu S, Tsubai-Shimizu S, Miyachi M, Iehara T and others. 2008. Effects of PAX3-FKHR on malignant phenotypes in alveolar rhabdomyosarcoma. Biochem Biophys Res Commun. p 568-74.

Kim WY, Sharpless NE. 2006. The Regulation of INK4/ARF in Cancer and Aging. 127(2):265-275.

Kunii K, Davis L, Gorenstein J, Hatch H, Yashiro M, Di Bacco A, Elbi C, Lutterbach B. 2008. FGFR2-Amplified Gastric Cancer Cell Lines Require FGFR2 and Erbb3 Signaling for Growth and Survival. Cancer Res 68(7):2340-2348.

Lagha M, Kormish J, Rocancourt D, Manceau M, Epstein J, Zaret K, Relaix F, Buckingham M. 2008. Pax3 regulation of FGF signaling affects the progression of embryonic progenitor cells into the myogenic program. Genes & Development. p 1828-1837.

Lam CW, Xie J, To KF, Ng HK, Lee KC, Yuen NW, Lim PL, Chan LY, Tong SF, McCormick F. 1999. A frequent activated smoothened mutation in sporadic basal cell carcinomas. Oncogene. p 833-6.

Langenau, Keefe, Storer, Guyon, Kutok, Le, Goessling, Neuberg, Kunkel, Zon. 2007. Effects of RAS on the genesis of embryonal rhabdomyosarcoma. Genes & Development. p 1382-1395.

Lee Y, Kawagoe R, Sasai K, Li Y, Russell HR, Curran T, McKinnon PJ. 2007. Loss of suppressor-of-fused function promotes tumorigenesis. Oncogene 26(44):6442-6447.

Liu W, Wu X, Zhang W, Montenegro RC, Fackenthal DL, Spitz JA, Huff LM, Innocenti F, Das S, Cook EH and others. 2007. Relationship of EGFR Mutations, Expression, Amplification, and Polymorphisms to Epidermal Growth Factor Receptor Inhibitors in the NCI60 Cell Lines. Clinical Cancer Research 13(22):6788-6795.

Lorusso P, Krishnamurthi S, Rinehart J, Nabell L, Malburg L, Chapman P, Deprimo S, Bentivegna S, Wilner K, Tan W and others. 2010. Phase I Pharmacokinetic and Pharmacodynamic Study of the Oral MAPK/ERK Kinase Inhibitor PD-0325901 in Patients with Advanced Cancers. Clinical Cancer Research. p 1924-1937.

Maher EA, Brennan C, Wen PY, Durso L, Ligon KL, Richardson A, Khatry D, Feng B, Sinha R, Louis DN and others. 2006. Marked genomic differences characterize primary and secondary glioblastoma subtypes and identify two distinct molecular and clinical secondary glioblastoma entities. Cancer Res. p 11502-13.

Malik KF, Jaffe H, Brady J, Young WS. 1997. The class III POU factor Brn-4 interacts with other class III POU factors and the heterogeneous nuclear ribonucleoprotein U. Brain Res Mol Brain Res. p 99-107.

Mao, Ligon, Rakhlin, Thayer, Bronson, Rowitch, Mcmahon. 2006. A Novel Somatic Mouse Model to Survey Tumorigenic Potential Applied to the Hedgehog Pathway. Cancer Res. p 10171-10178.

Martinelli S, McDowell HP, Vigne SD, Kokai G, Uccini S, Tartaglia M, Dominici C. 2009. RAS signaling dysregulation in human embryonal Rhabdomyosarcoma. Genes Chromosomes Cancer. p 975-82.

McEvilly RJ, de Diaz MO, Schonemann MD, Hooshmand F, Rosenfeld MG. 2002. Transcriptional regulation of cortical neuron migration by POU domain factors. Science. p 1528-32.

Mohammadi M, Froum S, Hamby JM, Schroeder MC, Panek RL, Lu GH, Eliseenkova AV, Green D, Schlessinger J, Hubbard SR. 1998. Crystal structure of an angiogenesis inhibitor bound to the FGF receptor tyrosine kinase domain. EMBO J 17(20):5896-5904.

Mullor JL, Dahmane N, Sun T, i Altaba AR. 2001. Wnt signals are targets and mediators of Gli function. 11(10):769-773.

Münsterberg, Kitajewski, Bumcrot, McMahon, Lassar. 1995. Combinatorial signaling by Sonic hedgehog and Wnt family members induces myogenic bHLH gene expression in the somite. Genes & Development. p 2911-22.

Network CGAR. 2008. Comprehensive genomic characterization defines human glioblastoma genes and core pathways. Nature 455(7216):1061-1068.

Oberlin O, Rey A, Lyden E, Bisogno G, Stevens MC, Meyer, Carli M, Anderson JR. 2008. Prognostic factors in metastatic rhabdomyosarcomas: results of a pooled analysis from United States and European cooperative groups. J Clin Oncol. p 2384-9.

Oeffinger KC, Mertens AC, Sklar CA, Kawashima T, Hudson MM, Meadows AT, Friedman DL, Marina N, Hobbie W, Kadan-Lottick NS and others. 2006.

Chronic health conditions in adult survivors of childhood cancer. N Engl J Med. p 1572-82.

Pandita, Zielenska, Thorner, Bayani, Godbout, Greenberg, Squire. 1999. Application of comparative genomic hybridization, spectral karyotyping, and microarray analysis in the identification of subtype-specific patterns of genomic changes in rhabdomyosarcoma. NEO. p 262-75.

Pollock PM, Gartside MG, Dejeza LC, Powell MA, Mallon MA, Davies H, Mohammadi M, Futreal PA, Stratton MR, Trent JM and others. 2007. Frequent activating FGFR2 mutations in endometrial carcinomas parallel germline mutations associated with craniosynostosis and skeletal dysplasia syndromes. Oncogene 26(50):7158-7162.

Pruitt SC, Bussman A, Maslov AY, Natoli TA, Heinaman R. 2004. Hox/Pbx and Brn binding sites mediate Pax3 expression in vitro and in vivo. Gene Expression Patterns 4(6):671-685.

Punyko JA, Mertens AC, Gurney JG, Yasui Y, Donaldson SS, Rodeberg DA, Raney RB, Stovall M, Sklar CA, Robison LL and others. 2005. Long-term medical effects of childhood and adolescent rhabdomyosarcoma: a report from the childhood cancer survivor study. Pediatr Blood Cancer. p 643-53.

Qualman, Coffin, Newton, Hojo, Triche, Parham, Crist. 1998. Intergroup Rhabdomyosarcoma Study: update for pathologists. Pediatr Dev Pathol. p 550-61.

Raaphorst FM. 2003. Self-renewal of hematopoietic and leukemic stem cells: a central role for the Polycomb-group gene Bmi-1. Trends Immunol. p 522-4.

Rand V, Huang J, Stockwell T, Ferriera S, Buzko O, Levy S, Busam D, Li K, Edwards JB, Eberhart C and others. 2005. Sequence survey of receptor tyrosine kinases reveals mutations in glioblastomas. Proceedings of the National Academy of Sciences of the United States of America 102(40):14344-14349.

Reis-Filho JS, Simpson PT, Turner NC, Lambros MB, Jones C, Mackay A, Grigoriadis A, Sarrio D, Savage K, Dexter T and others. 2006. FGFR1 Emerges as a Potential Therapeutic Target for Lobular Breast Carcinomas. Clinical Cancer Research 12(22):6652-6662.

Sahadevan K, Darby S, Leung HY, Mathers ME, Robson CN, Gnanapragasam VJ. 2007. Selective over-expression of fibroblast growth factor receptors 1 and 4 in clinical prostate cancer. The Journal of Pathology 213(1):82-90.

Sangha N, Wu R, Kuick R, Powers S, Mu D, Fiander D, Yuen K, Katabuchi H, Tashiro H, Fearon ER and others. 2008. Neurofibromin 1 (NF1) defects are common in human ovarian serous carcinomas and co-occur with TP53 mutations. NEO. p 1362-72, following 1372.

Scalzone M, Coccia P, Ruggiero A, Lazzareschi I, Mastrangelo S, Riccardi R. 2009. The Neurofibromatosis type 1:A dominantly inherited tumors-predisposing disorder. Cent Eur J Med. p 11-16.

Schaaf G, Hamdi M, Zwijnenburg D, Lakeman A, Geerts D, Versteeg R, Kool M. 2010. Silencing of SPRY1 Triggers Complete Regression of Rhabdomyosarcoma Tumors Carrying a Mutated RAS Gene. Cancer Res 70(2):762-771.

Sharp, Recio, Jhappan, Otsuka, Liu, Yu, Liu, Anver, Navid, Helman and others. 2002. Synergism between INK4a/ARF inactivation and aberrant HGF/SF signaling in rhabdomyosarcomagenesis. Nat Med. p 1276-80.

Shivakumar L, Minna J, Sakamaki T, Pestell R, White MA. 2002. The RASSF1A Tumor Suppressor Blocks Cell Cycle Progression and Inhibits Cyclin D1 Accumulation. Mol. Cell. Biol. 22(12):4309-4318.

Solit DB, Garraway LA, Pratilas CA, Sawai A, Getz G, Basso A, Ye Q, Lobo JM, She Y, Osman I and others. 2006. BRAF mutation predicts sensitivity to MEK inhibition. Nature 439(7074):358-362.

Stevens MC, Rey A, Bouvet N, Ellershaw C, Flamant F, Habrand JL, Marsden HB, Martelli H, Sanchez de Toledo J, Spicer RD and others. 2005. Treatment of nonmetastatic rhabdomyosarcoma in childhood and adolescence: third study of the International Society of Paediatric Oncology--SIOP Malignant Mesenchymal Tumor 89. J Clin Oncol. p 2618-28.

Storlazzi CT, Steyern FVV, Domanski HA, Mandahl N, Mertens F. 2005. Biallelic somatic inactivation of the <I>NF1</I> gene through chromosomal translocations in a sporadic neurofibroma. International Journal of Cancer 117(6):1055-1057.

Stratton MR, Fisher C, Gusterson BA, Cooper CS. 1989. Detection of point mutations in N-ras and K-ras genes of human embryonal rhabdomyosarcomas using oligonucleotide probes and the polymerase chain reaction. Cancer Res. p 6324-7.

Subramanian A, Tamayo P, Mootha VK, Mukherjee S, Ebert BL, Gillette MA, Paulovich A, Pomeroy SL, Golub TR, Lander ES and others. 2005. Gene set enrichment analysis: a knowledge-based approach for interpreting genome-wide expression profiles. Proc Natl Acad Sci USA. p 15545-50.

Subramanian S, Lui WO, Lee CH, Espinosa I, Nielsen TO, Heinrich MC, Corless CL, Fire AZ, van de Rijn M. 2008. MicroRNA expression signature of human sarcomas. Oncogene. p 2015-26.

Sugitani Y, Nakai S, Minowa O, Nishi M, Jishage K, Kawano H, Mori K, Ogawa M, Noda T. 2002. Brn-1 and Brn-2 share crucial roles in the production and positioning of mouse neocortical neurons. Genes & Development. p 1760-5.

Sung L, Anderson, Arndt C, Raney RB, Meyer, Pappo AS. 2004. Neurofibromatosis in children with Rhabdomyosarcoma: a report from the Intergroup Rhabdomyosarcoma study IV. J Pediatr. p 666-8.

Taipale J, Beachy PA. 2001. The Hedgehog and Wnt signalling pathways in cancer. Nature 411:349 - 354.

Taipale J, Chen JK, Cooper MK, Wang B, Mann RK, Milenkovic L, Scott MP, Beachy PA. 2000. Effects of oncogenic mutations in Smoothened and Patched can be reversed by cyclopamine. Nature 406(6799):1005-1009.

Tawbi H, Nimmagadda N. 2009. Targeted therapy in melanoma. Biologics. p 475-84.

Taylor AC, Shu L, Danks MK, Poquette CA, Shetty S, Thayer MJ, Houghton PJ, Harris LC. 2000. p53 mutation and MDM2 amplification frequency in pediatric rhabdomyosarcoma tumors and cell lines. Medical and Pediatric Oncology 35(2):96-103.

Taylor JG, Cheuk AT, Tsang PS, Chung JY, Song YK, Desai K, Yu, Chen QR, Shah K, Youngblood V and others. 2009. Identification of FGFR4-activating mutations in human rhabdomyosarcomas that promote metastasis in xenotransplanted models. J Clin Invest. p 3395-407.

Torkamani A, Schork NJ. 2008. Prediction of Cancer Driver Mutations in Protein Kinases. Cancer Res 68(6):1675-1682.

Tostar, Malm, Meis-Kindblom, Kindblom, Toftgård, Undén. 2005. Deregulation of the hedgehog signalling pathway: a possible role for thePTCH andSUFU genes in human rhabdomyoma and rhabdomyosarcoma development. J. Pathol. p 17-25.

Tsumura H, Yoshida T, Saito H, Imanaka-Yoshida K, Suzuki N. 2006. Cooperation of oncogenic K-ras and p53 deficiency in pleomorphic rhabdomyosarcoma development in adult mice. Oncogene. p 7673-9.

Valk-Lingbeek ME, Bruggeman SW, van Lohuizen M. 2004. Stem cells and cancer; the polycomb connection. Cell. p 409-18.

Vogel KS, El-Afandi M, Parada LF. 2000. Neurofibromin Negatively Regulates Neurotrophin Signaling through p21ras in Embryonic Sensory Neurons. Molecular and Cellular Neuroscience 15(4):398-407.

Vogel KS, Klesse LJ, Velasco-Miguel S, Meyers K, Rushing EJ, Parada LF. 1999. Mouse Tumor Model for Neurofibromatosis Type 1 . Science 286(5447):2176-2179.

Williamson D, Missiaglia E, De Reynies A, Pierron G, Thuille B, Palenzuela G, Thway K, Orbach D, Lae M, Freneaux P and others. 2010. Fusion Gene-Negative Alveolar Rhabdomyosarcoma Is Clinically and Molecularly Indistinguishable From Embryonal Rhabdomyosarcoma. Journal of Clinical Oncology. p 1-24.

Wolter M, Reifenberger J, Sommer C, Ruzicka T, Reifenberger G. 1997. Mutations in the Human Homologue of the Drosophila Segment Polarity Gene patched (PTCH) in Sporadic Basal Cell Carcinomas of the Skin and Primitive Neuroectodermal Tumors of the Central Nervous System. Cancer Res 57(13):2581-2585.

Xia, Holder DD, Pawel BR, Zhang C, Barr. 2009. High expression of the PAX3-FKHR oncoprotein is required to promote tumorigenesis of human myoblasts. Am J Pathol. p 2600-8.

Xia, Pressey, Barr. 2002. Molecular pathogenesis of rhabdomyosarcoma. Cancer Biol Ther. p 97-104.

Xie J, Johnson RL, Zhang X, Bare JW, Waldman FM, Cogen PH, Menon AG, Warren RS, Chen L-C, Scott MP and others. 1997. Mutations of the PATCHED Gene in Several Types of Sporadic Extracutaneous Tumors. Cancer Res 57(12):2369-2372.

Zwick E, Bange J, Ullrich A. 2002. Receptor tyrosine kinases as targets for anticancer drugs. Trends in Molecular Medicine 8(1):17-23.